Value-at-Risk Estimation: A Copula-GARCH Approach

Master's Thesis

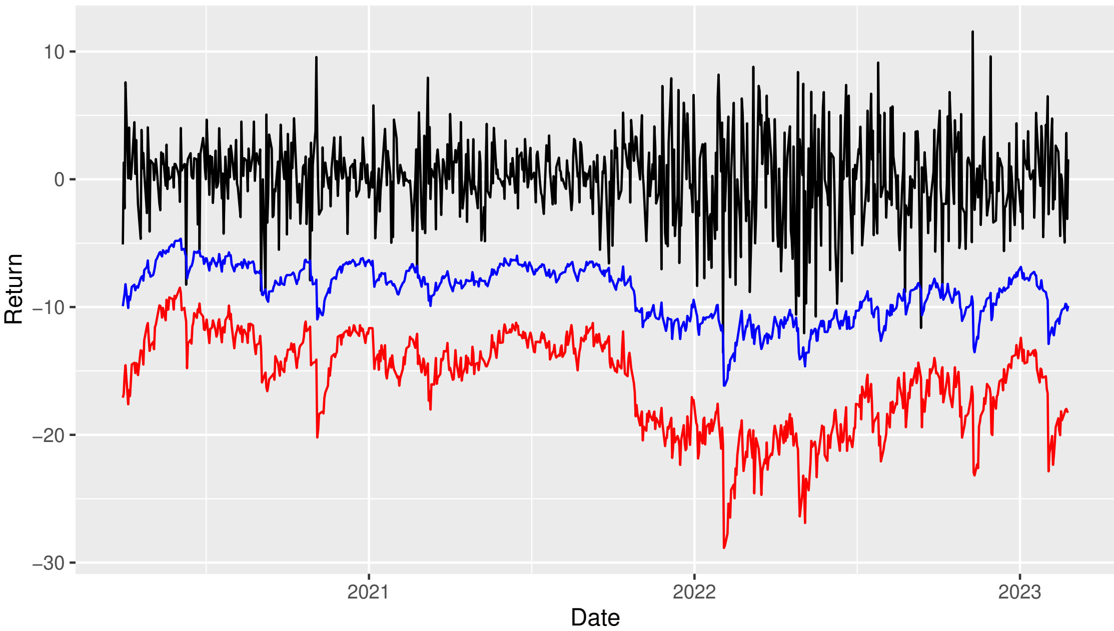

Financial Engineering

Mathematics-Economics

Kirstine Lykke Sørensen

Supervisor: Orimar Sauri

Submission date: 02/06/2023

AALBORG UNIVERSITY

STUDENT REPORT

Aalborg University

School of Engineering and Science

This document is typeset with LaTeX. Programming is performed in R.

AALBORG UNIVERSITY
STUDENT REPORT

School of Engineering and Science
Mathematics-Economics
Skjernvej 4A
9220 Aalborg Øst
http://math.aau.dk

Title:

Value-at-Risk Esimtation:
A Copula-GARCH Approach

Theme:

Master's Thesis

Project Period:

01/02 - 02/06/2023

Participant:

Kirstine Lykke Sørensen

Supervisor:

Orimar Sauri

Page Numbers: 79

Submission Date: 02/06/2023

Abstract:

The fundamental subject of this project is Value-at-Risk estimation of copula-GARCH models. The project investigates different estimation and evaluation methods of the Value-at-Risk of an equally weighted portfolio consisting of the 10 largest assets from the S&P500 index as of the 28th of February 2023. The purpose of the analysis is to determine which copula-GARCH model results in the best Value-at-Risk estimation based on multiple backtesting techniques. The analysis is made by introducing theory regarding copula models including definitions, properties, and examples as well as calibration methods. Moreover, risk measurements are defined and multiple estimation and evaluation techniques are presented. The data in the application contains the 10 assets' daily closing prices in the period from the 1st of June 2012 until the 27th of February 2023 as well as the daily closing prices of the S&P500 index in the period from the 1st of May 2013 until the 27th of February 2023. The data will be examined by use of the described copula-GARCH models, including data description, fitting of marginal distributions and copulas, Value-at-Risk estimation and evaluation, as well as coding in `R`.

Preface

This Master's Thesis in written in the Spring Semester of 2023 by Kirstine Lykke Sørensen, a student in Mathematics and Economics at the Department of Mathematical Sciences, Aalborg University.

There will be referred to sources with *[last name, year, pages/chapters]*. These are listed in alphabetical order in the bibliography. If a whole chapter or section is based on the source, it will be mentioned initially. If the source is mentioned before a period, it refers to the definition or sentence immediately before.

The code used in the application in Chapter 4 and 5 can be found on GitHub, see *[Sørensen, 2023]*. The coding has been done in `R`.

The author would like to extend her gratitude to the supervisor Orimar Sauri for his exquisite guidance throughout the completion of this project.

Signatures

Kirstine Lykke Sørensen

Contents

1 Introduction

For the last three years, the situation of the world has been very uncertain. First, in 2020 the COVID-19 pandemic shook the world [Bluemel and Henley, 2021]. The massive health crisis and the following lockdowns resulted in multiple industries closing, people being laid off, and a general uncertainty towards the future, both in terms of health and economy. Later, on the 24th of February 2022, Russia invaded Ukraine resulting in sanctions as well as much uncertainty on the gas market. In September 2022 the bombing of the Nordstream pipelines further supported these struggles. Both the COVID-19 pandemic and the uncertainty referring to Russia's invasion of Ukraine have affected the global economy greatly and the uncertainty in the economic market has risen. The aftermath of the events has caused a spike in the inflation and unemployment rates as well as a lot of companies going bankrupt, which has reduced the production capacity [Economics, 2021].

These events, and the financial influence they have had on the world in regards to job loss, reduced salary incomes, and general uncertainty among businesses, have made it more popular to invest in order to seek safety and wealth preservation [Bilimoria, 2021]. A popular investment approach is to base one's investment choices on the S&P500 index. This index features the 500 leading U.S. publicly traded companies. Because of the index's depth and diversity, it is widely considered one of the best gauges of the entire equities market [Kenton, 2023].
However, when investing, one of the most important things to consider is the risk of your investment. One of the most popular risk measurements is the Value-at-Risk, which quantifies how much capital one can assume to lose in a given period and with a given probability [Lu et al., 2011]. The measure is used to compare different investments and the goal is to minimize the expected loss at the given probability level. Often, the 95% Value-at-Risk and the 99% Value-at-Risk are observed.

The economic uncertainty of the world has resulted in the S&P500 index being very volatile in the last three years. This can be observed in the below figure which shows the prices of the index from the 1st of January 2020 until the 27th of February 2023.

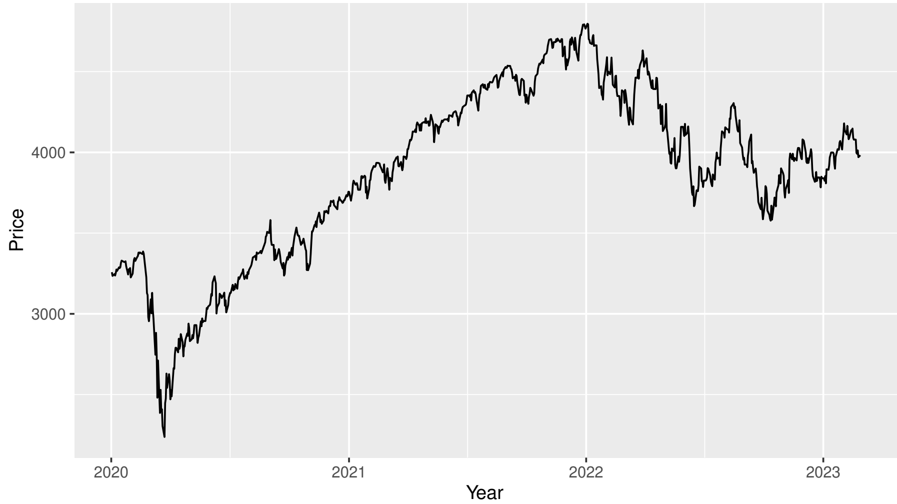

Figure 1.1: Prices of the S&P500 Index from 1st of January 2020 until 27th of February 2023

A common approach to modelling the volatility of the prices is by ARMA-GARCH models. These models are appropriate for time series data where the variance of the error term is serially autocorrelated and follows an autoregressive moving average process. Moreover, ARMA-GARCH models are useful to assess risk for assets that exhibit clustered periods of volatility in returns [Ruppert and Matteson, 2015].

When observing risk, it is always of interest to limit the risk of the investment. This is most often done by diversifying one's investment, e.g. by observing an index such as the S&P500 index and investing in multiple assets from the index. However, since this index contains 500 different assets, investments based on the index can require investing in a lot of different assets. This is not always beneficial, e.g. in regard to the requirement of a large initial capital as well as the fact that it is very time-consuming to invest in many assets. A way of dealing with these disadvantages is by constructing a smaller portfolio based on only a fraction of the assets from the index. It is then possible to analyze the portfolio by modelling the joint distribution of the assets by copula models. A common approach when building portfolios consisting of volatile assets is to make use of copula-GARCH models, e.g. as proposed by [Lu et al., 2011] and [Huang and So, 2018]. Thus, the marginal distributions of the copulas are modelled by ARMA-GARCH models in order to capture the volatility of the individual assets in the portfolio.

Thus, this project seeks to examine the Value-at-Risk of a portfolio based on copula-GARCH models. This leads to the following problem statement:

Problem Statement

How can the Value-at-Risk be used to evaluate an equally weighted portfolio based on copula-GARCH theory? Moreover, how do the Value-at-Risk models of the portfolio compare to the Value-at-Risk estimation of the S&P500 index?

The project seeks to answer the above problem statement by first introducing relevant theory regarding copulas. This theory includes definitions and examples of copulas, a description of tail dependence, and calibration of copulas. Afterwards, the Value-at-Risk is defined and different estimation and evaluation methods are presented. Next, the presented theory is applied to the daily closing prices of an equally weighted portfolio consisting of the 10 largest assets of the S&P500 index as of the 28th of February 2023. This is done on data from three different periods; first, the full period consisting of daily closing prices in the period from the 1st of June 2012 until the 27th of February 2023, afterwards in the period from the 1st of June 2012 until the 31st of March 2020 and lastly in the period from the 1st of April 2020 until the 27th of February 2023. Finally, the found Value-at-Risk models of the portfolio are compared to the Value-at-Risk estimation of the S&P500 index in the period from the 1st of May 2013 until the 27th of February 2023.

Copulas 2

This chapter is based on [Nelsen, 2006, pp. 7-46] and [Ruppert and Matteson, 2015, Chapter 8].

Copulas are used to define a framework for multivariate distributions and modelling of multivariate data. The copula of a multidimensional random vector, or more specifically of its distribution, is a function characterizing the dependence structure, thus the characteristics of its distribution, which do not depend on the margins. However, they can be combined with any set of univariate marginal distributions to form a joint distribution. Thus, copulas are widely used in regard to the construction of univariate models for multivariate data.

Before being able to formally define copulas, some important notation should be introduced. For any positive integer n, let $\bar{\mathbb{R}}^n$ denote the extended n-space $\bar{\mathbb{R}} \times \bar{\mathbb{R}} \times \cdots \times \bar{\mathbb{R}}$. For $\mathbf{a} \leq \mathbf{b}$ let $[\mathbf{a}, \mathbf{b}]$ denote the n-box $B = [a_1, b_1] \times [a_2, b_2] \times \cdots \times [a_n, b_n]$. The vertices of an n-box B are the points $\mathbf{c} = (c_1, c_2, \ldots, c_n)$ where each c_k is equal to either a_k or b_k. An n-place real function H is a function whose domain, $\mathrm{Dom}(H)$, is a subset of $\bar{\mathbb{R}}^n$ and whose range, $\mathrm{Ran}(H)$, is a subset of $\mathbb{R}$. Moreover, the unit n-cube $\mathbf{I}^n$ denotes the product $\mathbf{I} \times \mathbf{I} \times \cdots \times \mathbf{I}$, where $\mathbf{I} = [0, 1]$.

First, the H-volume of an n-box can be defined.

Definition 2.1.
Let $S_1, S_2, \ldots, S_n$ be nonempty subsets of $\bar{\mathbb{R}}$, and let H be an n-place real function such that $\mathrm{Dom}(H) = S_1 \times S_2 \times \cdots \times S_n$. Let $B = [\mathbf{a}, \mathbf{b}]$ be an n-box all of whose vertices are in $\mathrm{Dom}(H)$. Then the H-volume of B is given by

$$V_H(B) = \sum \mathrm{sign}(c) H(c), \tag{2.1}$$

where the sum is taken over all vertices of $\mathbf{c}$ of B, and

$$\mathrm{sign}(c) = \begin{cases} 1 & \text{if } c_k = a_k \text{ for an even number of } k\text{'s.} \\ -1 & \text{if } c_k = a_k \text{ for an odd number of } k\text{'s.} \end{cases} \tag{2.2}$$

The knowledge of the H-volume of a box is used in the following definition regarding n-increasing functions:

Definition 2.2.
An n-place real function H is n-increasing if $V_H(B) \geq 0$ for all n-boxes B whose vertices lie in $\mathrm{Dom}(H)$. Suppose that the domain of an n-place real function H is given by $\mathrm{Dom}(H) = S_1 \times S_2 \times \cdots \times S_n$, where each S_k has a least element a_k. Then H is grounded if $H(\mathbf{t}) = 0, \forall \mathbf{t} \in \mathrm{Dom}(H)$, such that $t_k = a_k$ for at least one k. If each S_k is nonempty and has a greatest element b_k, then H is said to have margins, and the one-dimensional margins of H are the functions H_k given by $\mathrm{Dom}(H_k) = S_k$, where

$$H_k(x) = H(b_1, \ldots, b_{k-1}, x, b_{k+1}, \ldots, b_n), \quad \forall x \in S_k. \tag{2.3}$$

Now that the definition of n-increasing functions is in place, subcopulas can be defined as below.

Definition 2.3.
An n-dimensional subcopula is a function C' with the following properties:

1. $\mathrm{Dom}(C') = S_1 \times S_2 \times \cdots \times S_n$, where each S_k is a subset of $\mathbf{I}$ containing 0 and 1,
2. C' is grounded and n-increasing,
3. C' has margins $C'_k, k = 1, 2, \ldots, n$, which satisfy

$$C'_k(u) = u, \quad \forall u \in S_k. \tag{2.4}$$

Next, copulas can be defined based on the definition of subcopulas. More specifically, n-dimensional real-valued copulas will be defined, which are generalized versions of real-valued n-dimensional subcopulas with domain $\mathbf{I}^n$.

Definition 2.4.
An n-dimensional copula is an n-subcopula C whose domain is $\mathbf{I}^n$. Equivalently, an n-copula is a function $C : [0,1]^n \to [0,1]$ that satisfies:

1. $C(u_1, \ldots, u_n) = 0$, whenever $u_i = 0$, for at least one $i = 1, \ldots, d$.
2. $C(u_1, \ldots, u_n) = u_i$, if $u_j = 1$, $\forall j = 1, \ldots, n$ and $j \neq i$.

3. For every $\mathbf{a}$ and $\mathbf{b}$ in $\mathbf{I}^n$ such that $\mathbf{a} \leq \mathbf{b}$,

$$V_C([\mathbf{a}, \mathbf{b}]) \geq 0.$$

This definition clarifies that a copula is a restriction to $[0,1]^n$ of a distribution function with uniform margins. Thus, considering a random variable $X : \Omega \to \mathbb{R}$ with continuous distribution $F_X : \mathbb{R} \to [0,1]$, then

$$\mathbb{P}(X \leq x) = F_X(x).$$

Based on this, a general result is that $F_X(x) \sim Unif(0,1)$. Consequently, $C_{\mathbf{Y}}$ contains all information on the dependencies of the components of $\mathbf{Y}$, however no information about the marginal CDFs of $\mathbf{Y}$. Since $C_{\mathbf{Y}}$ is the CDF of $\{F_{Y_1}(Y_1), \ldots, F_{Y_n}(Y_n)\}$, it holds that

$$\begin{aligned} C_{\mathbf{Y}}(u_1, \ldots, u_n) &= \mathbb{P}(F_{Y_1}(Y_1) \leq u_1, \ldots, F_{Y_n}(Y_n) \leq u_n) \\ &= \mathbb{P}\left(Y_1 \leq F_{Y_1}^{-1}(u_1), \ldots, Y_n \leq F_{Y_n}^{-1}(u_n)\right) \\ &= F_{\mathbf{Y}}\left(F_{Y_1}^{-1}(u_1), \ldots, F_{Y_n}^{-1}(u_n)\right). \end{aligned} \tag{2.5}$$

If $u_j = F_{Y_j}(y_j)$ for $j = 1, 2, \ldots, n$ then (2.5) results in

$$F_{\mathbf{Y}}(y_1, \ldots, y_n) = C_{\mathbf{Y}}(F_{Y_1}(y_1), \ldots, F_{Y_n}(y_n)). \tag{2.6}$$

This leads to the following important result:

Theorem 2.1 (Sklar's Theorem).
Let H be an n-dimensional distribution function with margins $F_1, F_2, \ldots, F_n$. Then there exists an n-copula C such that for all $\mathbf{x} \in \bar{\mathbb{R}}^n$,

$$H(x_1, x_2, \ldots, x_n) = C(F_1(x_1), F_2(x_2), \ldots, F_n(x_n)). \tag{2.7}$$

If $F_1, F_2, \ldots, F_n$ are all continuous, then C is unique. Otherwise, C is uniquely determined on $Ran(F_1) \times Ran(F_2) \times \cdots \times Ran(F_n)$. Conversely, if C is an n-copula and $F_1, F_2, \ldots, F_n$ are distribution functions, then the function H defined by (2.7) is an n-dimensional distribution function with margins $F_1, F_2, \ldots, F_n$.

Thus, Sklar's Theorem states that a random vector $\mathbf{Y}$ can be expressed as its copula $C_{\mathbf{Y}}$, which contains all information about the dependencies among $(Y_1, \ldots, Y_n)$, and its marginals $F_{Y_j}(y_j)$, which contain all information about the univariate marginal distributions.

2.1 Examples of Copulas

In this section, multiple examples of copulas will be presented. These copulas will be used in the application to find which one provides the best fit for the chosen data. First, Gaussian and t-copulas are presented, and afterwards, four different Archimedean copulas are defined.

Gaussian and t-Copulas

It can be useful to generate families of copulas which are based on multivariate normal and multivariate t-distributions. Let $\mathbf{Y} = (Y_1, \ldots, Y_n)$ have a multivariate normal distribution. As $C_{\mathbf{Y}}$ only depends on the dependencies within $\mathbf{Y}$, it only depends on the $n \times n$ correlation matrix of $\mathbf{Y}$, noted $\mathbf{\Omega}$. Thus, there is a correspondence between correlation matrices and Gaussian copulas. The Gaussian copula with correlation matrix $\mathbf{\Omega}$ is noted $C_{Gauss}(u_1, \ldots, u_n \mid \mathbf{\Omega})$ and is defined as below.

Definition 2.5.
Let $F(\cdot)$ denote the CDF of a univariate normal distribution. The n-dimensional Gaussian copula with covariance matrix $\mathbf{\Omega}$ is given by

$$C_{Gauss}(u_1, \ldots, u_n \mid \mathbf{\Omega}) = F_{Gauss}(F^{-1}(u_1), \ldots, F^{-1}(u_n)),$$

where F_{Gauss} is the CDF of the n-dimensional Gaussian distribution with mean 0 and covariance matrix $\mathbf{\Omega}$.

A random vector is said to have a meta-Gaussian distribution if it has a Gaussian copula.

The copula $C_t(u_1, \ldots, u_n \mid \mathbf{\Omega}, \nu)$ is the copula of a random vector which has a multivariate t-distribution with tail index ν and correlation matrix $\mathbf{\Omega}$. The tail index ν affects both the univariate marginal distributions and the tail dependence between the components. Thus, ν is also a parameter of C_t. The t-copula is defined below.

Definition 2.6.
Let t_ν denote the CDF of a univariate t-distribution with ν degrees of freedom. The n-dimensional t-copula with covariance matrix $\mathbf{\Omega}$ and ν degrees of freedom is given by

$$C_t(u_1, \ldots, u_n \mid \mathbf{\Omega}, \nu) = t_{\nu,\mathbf{\Omega}}(t_\nu^{-1}(u_1), \ldots, t_\nu^{-1}(u_n)),$$

where $t_{\nu,\mathbf{\Omega}}$ is the CDF of an n-dimensional t-distribution.

In the same manner, as the Gaussian copula, a random vector that has a t-copula is said to have a meta-t distribution.

Archimedean Copulas

This section is based on [Huang et al., 2009, pp. 317-318].

Archimedean copulas are widely used in applications, as they are easy to construct, have a great variety of different families, and possess many nice properties. Moreover, they have explicit expressions, which is of particular interest in applications. The definition of an Archimedean copula is given below.

Definition 2.7.
An Archimedean copula with a strict generator has the form

$$C(u_1, \dots, u_n) = \varphi^{-1}\{\varphi(u_1) + \cdots + \varphi(u_n)\}, \tag{2.8}$$

where the generator function φ satisfies:

1. It is a continuous, strictly decreasing and convex function, that maps $[0, 1]$ onto $[0, \infty]$,
2. $\varphi(0) = \infty$,
3. $\varphi(1) = 0$.

Below, four different families of Archimedean copulas will be described.

Clayton Copula

The Clayton copula has the generator function

$$\varphi_{Cl}(u \mid \theta) = \frac{1}{\theta}(u^{-\theta} - 1), \quad \theta > 0,$$

and is thus given on the form

$$C_{Cl}(u_1, \dots, u_d \mid \theta) = (u_1^{-\theta} + \cdots + u_d^{-\theta} + 1 - d)^{-\frac{1}{\theta}}.$$

Frank Copula

The generator of the Frank copula is given as

$$\varphi_{Fr}(u \mid \theta) = -\log\left(\frac{e^{-\theta u} - 1}{e^{-\theta} - 1}\right), \quad -\infty < \theta < \infty.$$

Thus the Frank copula is given on the form

$$C_{Fr}(u_1,\ldots,u_d \mid \theta) = -\frac{1}{\theta}\log\left(1+\frac{(e^{-\theta u_1}-1)\ldots(e^{-\theta u_2}-1)}{(e^{-\theta}-1)^{d-1}}\right).$$

Gumbel Copula

The Gumbel copula has the generator function

$$\varphi_{Gu}(u \mid \theta) = (-\log(u))^{\theta}, \quad \theta \geq 1,$$

and is given on the form

$$C_{Gu}(u_1,\ldots,u_d \mid \theta) = \exp\left(-\left\{(-\log(u_1))^{\theta}+\cdots+(-\log(u_d))^{\theta}\right\}^{\frac{1}{\theta}}\right).$$

Joe Copula

The generator function of the Joe copula is given on the form

$$\varphi_{Joe}(u \mid \theta) = -\log\left\{1-(1-u)^{\theta}\right\}, \quad \theta \geq 1.$$

Thus, the Joe copula is given as

$$C_{Joe}(u_1,\ldots,u_d \mid \theta) = 1-\left[1-(1-(1-u_1)^{\theta})\ldots(1-(1-u_d))^{\theta}\right]^{\frac{1}{\theta}}.$$

2.2 Tail Dependence

This section is based on [Nelsen, 2006, pp. 214-216] and [Ruppert and Matteson, 2015, pp. 196-198].

In risk management, it is of great use to be able to measure tail dependence, which is the dependence between the variables in the upper-right quadrant and the lower-left quadrant of $\mathbf{I}^2$. If the returns of assets in a given portfolio do not have any tail dependence among them, then there will be little risk of simultaneous very negative returns. The converse holds if tail dependence is present.

The tail dependence is evaluated based on the upper and lower tail dependence parameters, λ_U and λ_L. Assume $\mathbf{Y} = (Y_1, Y_2)$ is a bivariate random vector with corresponding copula C_Y. Then the coefficient of lower tail dependence, λ_L, is defined as

$$
\begin{aligned}
\lambda_L &= \lim_{q \downarrow 0} \mathbb{P}\left\{Y_2 \leq F_{Y_2}^{-1}(q) \mid Y_1 \leq F_{Y_1}^{-1}(q)\right\} \\
&= \lim_{q \downarrow 0} \frac{\mathbb{P}\left\{Y_1 \leq F_{Y_1}^{-1}(q), Y_2 \leq F_{Y_2}^{-1}(q)\right\}}{\mathbb{P}\left\{Y_1 \leq F_{Y_1}^{-1}(q)\right\}} \\
&= \lim_{q \downarrow 0} \frac{\mathbb{P}\left\{F_{Y_1}(Y_1) \leq q, F_{Y_2}(Y_2) \leq q\right\}}{\mathbb{P}\left\{F_{Y_1}(Y_1) \leq q\right\}} \\
&= \lim_{q \downarrow 0} \frac{C_Y(q,q)}{q}.
\end{aligned}
$$

In the above, it is assumed that F_{Y_1} and F_{Y_2} are strictly increasing on their supports, such that their inverses exist. Since λ_L is defined as the conditional probability of $Y_2 \leq F_{Y_2}^{-1}(q)$, it holds that if $\lambda_L = 0$, then Y_1 and Y_2 act as if they are independent in the extreme left tail.

The coefficient of upper tail dependence, λ_U, is defined as

$$
\begin{aligned}
\lambda_u &= \lim_{q \uparrow 1} \mathbb{P}\left\{Y_2 \geq F_{Y_2}^{-1}(q) \mid Y_1 \geq F_{Y_1}^{-1}(q)\right\} \\
&= 2 - \lim_{q \uparrow 1} \frac{1 - C_Y(q,q)}{1-q}.
\end{aligned}
$$

The above is defined analogously to λ_L, thus λ_U is the limit as $q \uparrow 1$ of the conditional probability.

In regards to the Normal and t-copula, special cases hold. Any bivariate Normal copula C_{Gauss} with $\rho \neq 1$, does not exhibit either lower or upper tail dependence. In regards to the bivariate t-copula C_t with ν degrees of freedom and correlation ρ, the formula for both the lower and upper tail dependence is given as

$$
\lambda_U = \lambda_L = 2F_{t,\nu+1}\left\{-\sqrt{\frac{(\nu+1)(1-\rho)}{1+\rho}}\right\},
$$

where $Ft, \nu + 1$ is the CDF of the t-distribution with $\nu + 1$ degrees of freedom. Since $F_{t,\nu+1}(-\infty) = 0$, it holds that $\lambda_L \to 0$ as $\nu \to \infty$.

Tail dependency is often observed in scatterplots of the different copulas. It appears as a spike in the data points in the upper-right or lower-left corner of the plot.

2.3 Calibrating Copulas

This section is based on [Cherubini et al., 2004, pp. 153-160].

In this section, two different methods will be presented, which are useful when determining which copula to work with. It will be assumed that $\{\mathbf{Y}_t, t \in \mathbb{Z}\}$ is a strictly stationary stochastic process taking values in $\mathbb{R}^d$. Moreover, it will be assumed that the data consists of a realization of n-dimensional real vectors $\{\mathbf{Y}_t, t = 1, 2, \ldots, T\}$.

Maximum Likelihood Estimation

Assume the parametric models for the marginal CDFs,

$$F_{Y_1}(\cdot \mid \boldsymbol{\theta}_1), \ldots, F_{Y_d}(\cdot \mid \boldsymbol{\theta}_n),$$

as well as a parametric model for the copula density, $c_Y(\cdot \mid \boldsymbol{\theta}_C)$, are given. Then, the log-likelihood is given as

$$\begin{aligned}\log\left\{L(\boldsymbol{\theta}_1, \ldots, \boldsymbol{\theta}_n, \boldsymbol{\theta}_C)\right\} = \sum_{i=1}^{d} \Big(&\log\left[c_Y\left\{F_{Y_1}(Y_{i,1} \mid \boldsymbol{\theta}_1), \ldots, F_{Y_n}(Y_{i,n} \mid \boldsymbol{\theta}_n) \mid \boldsymbol{\theta}_C\right\}\right] \\ &+ \log\left\{f_{Y_1}(Y_{i,1} \mid \boldsymbol{\theta}_1)\right\} + \cdots + \log\left\{f_{Y_n}(Y_{i,n} \mid \boldsymbol{\theta}_n)\right\} \Big).\end{aligned}$$

However, a disadvantage of this method is that it can be very computationally intensive, especially in the case of high dimensions. This is the case, as it is necessary to jointly estimate the parameters of the marginal distribution and the parameters of the dependence structure represented by the copula.

Inference Function For Margins

An alternative to the maximum likelihood estimation method given above, which is not as computationally burdensome, is the inference for margins (IFM) method. This method involves estimating the parameters of the margin and the copula density in two steps instead of jointly:

1. First, estimate the margins' parameters $\hat{\boldsymbol{\theta}}_m = [\hat{\boldsymbol{\theta}}_1, \ldots, \hat{\boldsymbol{\theta}}_n]^\mathsf{T}$ by performing the estimation of the univariate marginal distributions:

$$\hat{\boldsymbol{\theta}}_m = \arg\max_{\boldsymbol{\theta}_m} \sum_{i=1}^{d} \left(\log\{f_{Y_1}(Y_{i,1} \mid \boldsymbol{\theta}_1)\} + \ldots + \log\{f_{Y_n}(Y_{i,n} \mid \boldsymbol{\theta}_n)\}\right).$$

2. Second, estimate the copula parameter $\boldsymbol{\theta}_C$ given $\hat{\boldsymbol{\theta}}_m$:

$$\hat{\boldsymbol{\theta}}_C = \arg\max_{\boldsymbol{\theta}_C} \sum_{i=1}^{d} \left(\log \left[c_Y \{ F_{Y_1}(Y_{i,1} \mid \boldsymbol{\theta}_1), \ldots, F_{Y_n}(Y_{i,n} \mid \boldsymbol{\theta}_n) \mid \boldsymbol{\theta}_C, \hat{\boldsymbol{\theta}}_m \} \right] \right).$$

The IFM estimator is then defined as the vector

$$\hat{\boldsymbol{\theta}}_{IFM} = \left(\hat{\boldsymbol{\theta}}_m, \hat{\boldsymbol{\theta}}_C \right)^{\mathsf{T}}.$$

Risk Measures 3

This chapter is based on [Ruppert and Matteson, 2015, pp. 553-565] and [Elliott and Kopp, 2005, pp. 303-315].

In this chapter, the Value-at-Risk will be described, which is one of the most commonly used risk measures. Moreover, different ways of estimating and evaluating the Value-at-Risk will be given. These methods are used in Chapter 4 and 5 to describe the risk of the constructed portfolio and the index fund.

3.1 Value-at-Risk

The idea behind Value-at-Risk, also denoted VaR, is to determine a level of exposure in a position that will not be exceeded. This level is determined based on a given threshold level $\alpha \in [0, 1]$, which can vary based on the given scenario and data. As α can be seen as a confidence level, it must hold that $\alpha \in [0, 1]$. Moreover, VaR also uses a time horizon, denoted T. Thus, VaR can be seen as a bound such that the loss over the horizon is less than this bound with probability equal to the confidence coefficient α.

If $\mathcal{L}$ denotes the loss over the holding period T, then VaR(α) is the αth upper quantile of $\mathcal{L}$. For continuous loss distributions,

$$\mathbb{P}(\mathcal{L} > VaR(\alpha)) = \mathbb{P}(\mathcal{L} \geq VaR(\alpha)) = \alpha,$$

and for any loss distribution,

$$VaR(\alpha) = \inf\{x : \mathbb{P}(\mathcal{L} > x) \leq \alpha\}.$$

Nevertheless, a disadvantage of VaR is that it is not subadditive. Thus, diversification of positions will not necessarily reduce risk.

3.2 Estimation of VaR

This section is based on [Ruppert and Matteson, 2015, Chapter 19], [Kuester et al., 2006, pp. 56-60] and [Choudhry, 2013, Chapter 3].

Value-at-Risk can be estimated by the use of multiple different methods. In this section, historical estimation and parametrical estimation will be given for an asset. In the following section, Monte Carlo estimation of VaR will be presented.

In the historical estimation, only the prior history of the returns is considered. Thus, there is no need to assume a parametric family, such as e.g. the normal distribution or t-distribution. The confidence level, α, is found by estimating the return distribution. This quantile is then estimated as the α-quantile of a sample of historic returns, which is denoted $\hat{q}(\alpha)$. Let S be the size of the current position. Then the historical estimate of VaR is

$$\widehat{VaR}^{hist}(\alpha) = -S \times \hat{q}(\alpha),$$

where the minus sign indicates that potential loss is returned rather than potential revenue.

Since the historical simulation uses historical data to calculate potential losses, and assumes that history will repeat itself, it is important to have a large data set to capture possible fluctuations or special events. However, an advantage of the historical method is the fact that it does not assume any distributions of the data and thus cannot misspecify any distributions.

Instead of assuming that the past will repeat itself, the parametric estimation method assumes that gains and losses are parametrically distributed, e.g. by assuming a jointly normal distribution or t-distribution. The volatilities and correlations can be calculated in two different ways. Either by assuming simple historical volatility, where each past observation is equally weighted in the volatility calculation, or by assigning different past observations different weights. The latter is often done by use of either GARCH models or exponentially weighted MA processes to assign the weights. The parametric estimation is also of great use in smaller sample sizes.

Let $F(y \mid \theta)$ be a parametric family of distributions used to model the return distribution and assume that $\hat{\theta}$ is an estimate of θ, e.g. the MLE computed from historic returns. Then $F^{-1}(\alpha \mid \hat{\theta})$ is an estimate of the α-quantile of the return distribution. In this case, a parametric estimate of $VaR(\alpha)$ is given as

$$\widehat{VaR}^{par}(\alpha) = -S \times F^{-1}(\alpha \mid \theta). \tag{3.1}$$

3.3 Monte Carlo Estimation

This section is based on [Lu et al., 2011, pp. 340-342].

In this section, a Monte Carlo procedure to forecast one-day ahead VaR is presented. Only equally weighted portfolios consisting of d assets are considered. From now on, the number of observations is noted as T, as time observations are observed. The daily log-returns of asset j are given as

$$r_t^j = \log\left(\frac{P_t^j}{P_{t-1}^j}\right) = \log(P_j) - \log(P_{t-1}^j), \quad j = 1, \ldots, d, \tag{3.2}$$

where P_t^j is the price of asset j at time t. The log-returns of the equally weighted portfolio at time t are then denoted as

$$r_t^P = \frac{1}{d}r_t^1 + \frac{1}{d}r_t^2 + \cdots + \frac{1}{d}r_t^d.$$

Denote the profit and loss (P&L) function of the portfolio composed of d assets at time t, by L_t, which is given as

$$\begin{aligned} L_t &= \frac{1}{d}P_t^1 + \cdots + \frac{1}{d}P_t^d - \left(\frac{1}{d}P_{t-1}^1 + \cdots + \frac{1}{2}P_{t-1}^d\right) \\ &= \frac{1}{d}P_{t-1}^1\left(\exp(r_t^1) - 1\right) + \cdots + \frac{1}{d}P_{t-1}^d\left(\exp(r_t^d) - 1\right). \end{aligned} \tag{3.3}$$

The procedure to forecast one-day-ahead VaR based on copulas at a 95% and a 99% confidence level is as follows:

1. Using T observations, ARMA-GARCH type models, described in Section 4.2, are fitted, and marginal distributions are estimated for each log-return series.

2. One-step means and variances, denoted $\hat{r}_{T+1}^j$ and $\hat{h}_{T+1}^j$ for $j = 1, \ldots, d$, are forecasted at time $T + 1$.

3. The copula parameters $\hat{\kappa}$ are estimated by use of the probability integral transforms $u_t^1, \ldots, u_t^d$ of the standardized residuals $\eta_t^1, \ldots, \eta_t^d$ of the ARMA-GARCH-type models.

4. The d random variables $(u_{T+1}^{1,k}, \ldots, u_{T+1}^{d,k})$ for $k = 1, 2, \ldots, N$ are simulated from the copula[1].

[1] The simulation methods of Normal copulas, t-copulas and Archimedean copulas are mentioned in [Hofert et al., 2018, pp. 86-90].

5. The simulated standardized residuals $\eta_{T+1}^{j,k}$, for $j = 1, \ldots, d$ and $k = 1, \ldots, N$ are obtained by use of the inverse functions of the estimated marginals,

$$\left(\eta_{T+1}^{1,k}, \ldots, \eta_{T+1}^{d,k}\right) = \left(F_{1,T+1}^{-1}(u_{T+1}^{1,k}; \hat{\boldsymbol{\theta}}_1), \ldots, F_{d,T+1}^{-1}(u_{T+1}^{d,k}; \hat{\boldsymbol{\theta}}_d)\right).$$

6. The simulated asset log-returns are obtained as

$$\left(r_{T+1}^{1,k}, \ldots, r_{T+1}^{d,k}\right) = \left(\hat{r}_{T+1}^{1} + \eta_{T+1}^{1,k} \cdot \sqrt{\hat{h}_{T+1}^{1}}, \ldots, \hat{r}_{T+1}^{d} + \eta_{T+1}^{d,k} \cdot \sqrt{\hat{h}_{T+1}^{d}}\right).$$

7. The values of L_{T+1}^k are calculated using (3.3) for $k = 1, \ldots, N$.

8. The N values of L_{T+1}^k are sorted in increasing order. Then the 95% VaR and 99% VaR are calculated as:
   i) The 95% VaR is the absolute value of the $N \times (1 - 95\%)$ ordered scenarios of L_{T+1}^k;
   ii) The 99% VaR is the absolute value of the $N \times (1 - 99\%)$ ordered scenario of L_{T+1}^k.

9. Repeat the above steps M times by rolling over the daily returns for a given time period with one-day increments. Let M be the number of out-of-samples instances. The 95% VaR and 99% VaR values are then used for backtesting as described in Section 3.4.

3.4 Backtesting

This section is based on [Lu et al., 2011, pp. 342-343], [Abad et al., 2014] and [Fantazzini, 2008].

After the forecasting of VaR for each day in the out-of-sample has been performed, the forecasted VaR estimates should be compared with the real observed portfolio P&L function. Afterwards, the performance of the constructed models should be evaluated using backtesting techniques. In this section, two statistical tests and two loss functions will be introduced in order to backtest the performance of different VaR models. These methods are used to evaluate the predictive performance of a model based on historical data.

Define the hit series I_t as

$$I_t = \begin{cases} 1 & \text{if } L_t < -VaR_t, \\ 0 & \text{if } L_t \geq -VaR_t, \end{cases} \quad \text{for } t = 1, \ldots, T, \tag{3.4}$$

where L_t is the observed P&L function. Thus, I_t is 1 when the value of the observed P&L function is less than the negative forecasted VaR threshold, and 0 otherwise. Moreover, define q as the true probability coverage and let $Z_T = \sum_{t=1}^{T} I_t$ be the number of exceptions in a sample size of size T. In the rest of the project Z_T will be denoted as Z however, still under the assumption that it is observed at time T.

The first statistical test is Kupiec's unconditional coverage test, which is based on binomial theory and tests the difference between the observed and the expected number of VaR exceptions of the effective portfolio profits and losses. Generally, the ratio of VaR exceedances is calculated as Z/T. Following the binomial theory, the probability of observing Z failures out of T observations is $(1-q)^{T-Z}q^Z$, so the null hypothesis, which is that the observed exception frequency Z is equal to the expected exceptions, is given by the likelihood ratio test statistic:

$$LR_{UC} = -2\log\left[(1-q)^{T-Z}q^Z\right] + 2\log\left[(1-Z/T)^{T-Z}(Z/T)^Z\right],$$

where $T-Z$ is the successes, Z is the failures and $(1-q)^{T-Z}(Z/T)^Z$ is the probability of having $T-Z$ successes. Thus, the test compares the predicted number of times VaR is exceeded against the observed number of times VaR is exceeded. In other words, whether $q = Z/T$. The test can reject a model for both high and low failures, however, it ignores conditioning or time variation in the data, and thus cannot cope with clustering in the observations. When T is large enough, this test statistic is asymptotically distributed as $\chi^2(1)$ under H_0, which indicates that the observed number of exceedings statistically equals the predicted number of exceedings. Note, that $(1-q)$ is the probability for the losses to exceed the VaR. Thus, if the losses exceed the VaR more frequently, the test underestimates the risk of the portfolio. Conversely, if the losses exceed the VaR less frequently the risk of the portfolio is overestimated.

An alternative approach to Kupiec's unconditional coverage test, which does not suffer from the above-mentioned shortcomings, is Christoffersen's conditional coverage test. This test tests the joint assumption of unconditional coverage and independence of failures. Under the null hypothesis, the independence results in a case where a violation at time t does not have any influence on the probability of violations at time $t+1$. The test statistic is given as

$$\begin{aligned} LR_{CC} &= LR_{UC} + LR_{IND} \\ &= -2\log\left[(1-q)^{T-Z}q^Z\right] + 2\log\left[(1-\pi_{01})^{n_{00}}\pi_{01}^{n_{01}}(1-\pi_{11})^{n_{10}}\pi_{11}^{n_{11}}\right], \end{aligned}$$

where n_{ij} denotes the number of transitions from state i to state j in the hit series I_t, for $i,j = 0,1$, and $\pi_{ij} = (n_{ij})/(\sum_j n_{ij})$ are the corresponding probabilities of the events. The probabilities are independent if $\pi_{01} = \pi_{11} = (1 - q)$. Where Kupiec's test restricts the number of allowed violations, Christoffersen's test further restricts the way the violations occur. Thus, it can reject a model for having too many or too few clustered violations. This test is distributed as $\chi^2(2)$ under H_0, which is that the probabilities of VaR exceedings are independent.

Both Kupiec's and Christoffersen's test statistics focus on examining the behaviour of the hit function. They choose acceptable models based on the number of exceptions and limit the information contained in the number of exceptions. Moreover, they do not show any power in distinguishing between different, but close, alternatives, which results in the construction of a general loss function equal to the hit series given in (3.4). However, multiple alternatives to the general loss function can be considered, which makes it possible to evaluate the non-covered losses. Thus, the following two loss functions are based on examining the distance between the observed returns and the forecasted VaR values when losses are uncovered.

The first loss function proposed by Lopez is given as

$$C_t^L = \begin{cases} 1 + (|L_t| - VaR_t)^2, & \text{if } L_t < -VaR_t, \\ 0, & \text{if } L_t \geq -VaR_t, \end{cases}$$

This measure includes an additional term based on the magnitude of an exception, except for the score of one when an exception occurs. The inclusion of the quadratic term ensures that large failures are penalized more than small failures. A backtest using this loss function would typically be based on the sample average loss,

$$\hat{C}^L = \frac{1}{T} \sum_{t=1}^{T} C_t^L.$$

Another alternative loss function is the one proposed by Bianco and Ihle, which focuses on the average size of exceptions,

$$C_t^{BI} = \begin{cases} \frac{|L_t| - VaR_t}{VaR_t}, & \text{if } L_t < -VaR_t, \\ 0, & \text{if } L_t \geq -VaR_t, \end{cases}$$

Thus, this loss function evaluates how well the VaR model performs on average. The backtesting using this loss function is similar to that of Lopez's loss function, thus

$$\hat{C}^{BI} = \frac{1}{T} \sum_{t=1}^{T} C_t^{BI}.$$

As the two proposed loss functions do incorporate the distance between the observed returns and the forecasted VaR values, they make it possible to rank the performance of different models to each other. When constructing the VaR models, the goal is to construct a model which most accurately illustrates the actual risk, thus the q level. Since $\hat{C}^L$ and $\hat{C}^{BI}$ measures the sum of the difference between the observed returns and the calculated VaR values, the lower the value of $\hat{C}$, the better goodness-of-fit of the proposed VaR model.

Application 4

In this chapter, the data application will be conducted. First, the chosen data for the construction of the portfolio will be presented and analyzed. Then marginal distributions of each of the chosen assets will be fitted. Afterwards, the portfolio will be constructed as a copula, which will be based on the theory presented in Section 2.1. Hereafter, the Value-at-Risk is forecasted using the Monte Carlo procedure introduced in Section 3.3 and evaluated based on the backtesting methods given in Section 3.4. This procedure will be performed for three different periods, namely the full sample, the train set, and the test set. Lastly, the copula-GARCH VaR forecasts for the full sample will be compared with the VaR forecasts of an index fund. This is done in order to investigate, which procedure results in the best-fitting model in regards to the Value-at-Risk performance.

4.1 Data Description

The data used for constructing the portfolio is collected from Yahoo Finance, and consists of daily closing prices in United States Dollars (USD), from now on denoted prices. The prices are observed in the period from the 1st of June 2012 until the 27th of February 2023, thus a total number of $2,802$ weekdays. As mentioned in Chapter 1, the application will be based on the S&P500 index. The 10 biggest assets of the S&P500 index as of the 28th of February 2023 were chosen to construct a portfolio. These 10 assets make up approximately 28% of the S&P500 index and are thus of significant influence on the behaviour of the whole index. The chosen assets are:

No.	Company	Symbol	Sector*	Weight %
1	Apple Inc.	AAPL	Information Technology	7.180
2	Microsoft Corp.	MSFT	Information Technology	6.292
3	Amazon.com Inc	AMZN	Consumer Discretionary	2.636
4	NVIDIA Corp.	NVDA	Information Technology	1.985
5	Alphabet Inc. A	GOOGL	Communication Services	1.892
6	Alphabet Inc. C	GOOG	Communication Services	1.659
7	Berkshire Hathaway B	BRK.B	Financials	1.622
8	Tesla Inc.	TSLA	Consumer Discretionary	1.543
9	Meta Platforms Inc. A	META	Communication Services	1.381
10	UnitedHealth Group Inc.	UNH	Health Care	1.340

Table 4.1: The 10 largest assets of the S&P500 index as of the 28th of February 2023 based on slickcharts.com/sp500
*Based on GICS sectors

From now on, whenever a portfolio is referred to, an equally weighted portfolio consisting of the 10 assets mentioned above is considered. Thus, from now on, they each take up 10% of the constructed portfolio instead of the previously mentioned weights.

The data is split into two parts; the train set and the test set. The train set consists of $2,043$ days, thus daily data from the 1st of June 2012 until the 31st of March 2020, whereas the test set consists of 759 observations, responding to daily data from the 1st of April 2020 until the 27th of February 2023. The price of the equally weighted portfolio is plotted below with the dotted line corresponding to the division between the train and test set:

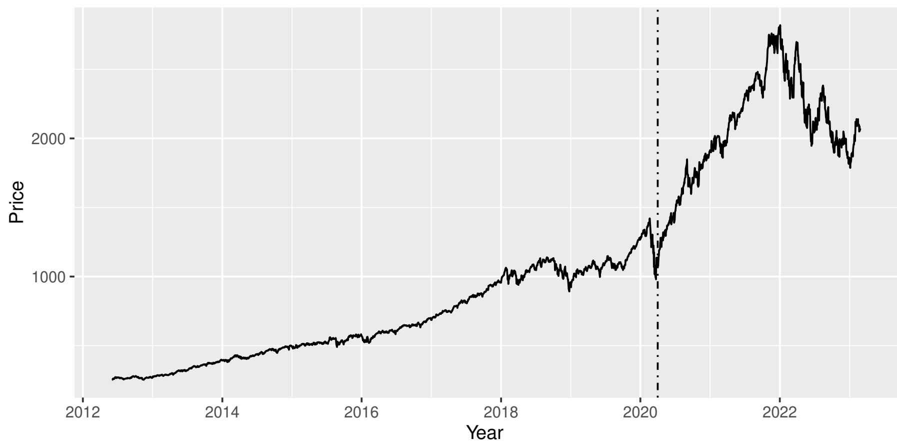

Figure 4.1: Portfolio prices from 1st of June 2012 until 27th of February 2023. The dotted line represents the division between the train and test set.

It can be seen, that the prices are increasing throughout the period, and especially in the first half of the test set. Moreover, it can be seen that the prices are relatively volatile, which is most obvious in 2022 and 2023, where a lot of big increases and decreases are seen. However, a large decrease is seen just around the division of the train and test set, which is most likely because of the corona crisis. This decline causes the train set to behave differently in the very last period compared to the rest of the train set, which will likely influence the model fitting later on. Moreover, it can be seen that the prices behave differently in the train and test set, which might influence the performance of the Value-at-Risk forecasts in Section 4.4.

To be able to fit ARMA-GARCH models on each of the 10 chosen assets, the daily prices are converted to log-returns, to ensure stationarity. The log-returns at time t, r_t, are computed by (3.2). The log-returns of each of the 10 assets are shown below for the full sample:

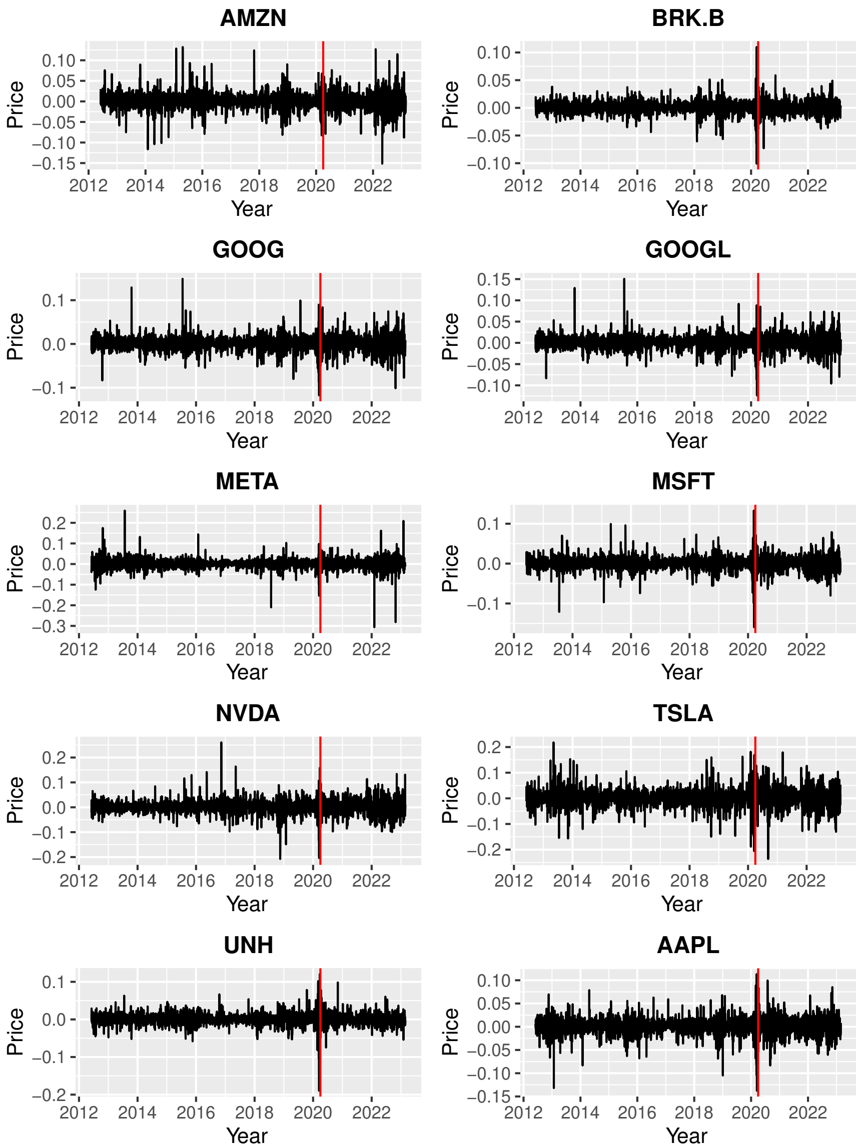

Figure 4.2: Log-returns from 1st of June 2012 until 27th of February 2023. The red lines represent the division between the train and test sets.

It can be seen that all of the log-returns seem relatively stationary around 0, however, they still possess a lot of volatility throughout all of the period. The most volatility is seen in the test set, which was expected from observing Figure 4.1. It can also be seen, that the fluctuations are larger for GOOGL, META, NVDA and TSLA than for the rest of the assets. Moreover, it can be seen that all of the assets, except AMZN and META, have the largest fluctuations around the beginning of 2020, which can also be observed from Figure 4.1.

Note that since the log-returns are observed, the train set shrunk with 1 observation. Thus, the train set now consists of daily log-returns in the period from the 2nd of June 2012 until the 31st of March 2023, which accounts for a total of $2,042$ observations.

To investigate the log-returns further, the descriptive statistics for both the full sample, the train set and the test set are given in Table 4.2. It can be seen from the table, that the means for all 10 assets are approximately 0 for all three samples, however, they are closer to 0 in the test set than in the train set. Moreover, the standard deviations are approximately the same for all 10 assets throughout all of the three samples.

The 95% and 99% VaR values are based on historical estimation, thus calculated purely on the past data without making assumptions about the parametric distributions. It can be seen, that both the 95% and 99% VaR values are negative for all 10 assets in all three periods, however, they are all relatively close to 0. Moreover, it can be seen that BRK.B has the highest 95% and 99% VaR for all three samples. On the other hand, TSLA is the asset with the lowest 95% and 99% VaRs, thus it is the asset in which one can expect with 95% and 99% certainty to lose the most.

Regarding the skewness of the assets, it can be seen that both positive and negative values are present, indicating both right-skewed and left-skewed data. It can be seen that META is the most skewed asset in the full sample and the test set, whereas UNH is the most skewed asset in the training set. The same behaviour is seen when observing the excess kurtosis where it can be seen that META has the heaviest tails in the full sample and test sample, and UNH has the heaviest tails in the training set. The Jarque-Bera test, which is a goodness-of-fit test described in Appendix A.1, rejects the null hypothesis of normally distributed data for all 10 assets in all three samples. Thus, neither of the log-returns are normally distributed. The ADF test supports the stationarity seen in Figure 4.2 as it rejects the null hypothesis of a unit root for all 10 assets in all three samples. Furthermore, the Ljung-Box test fails to reject the null hypothesis of independently distributed data for AMZN and TSLA for both the full sample and the train set, however, it only rejects the null hypothesis for MSFT in the test set. Thus, in the full set and training set most of the assets have autocorrelation, whereas most of the assets are independently distributed in the test set.

Full Sample	**AMZN**	**BRK.B**	**GOOG**	**GOOGL**	**META**	**MSFT**	**NVDA**	**TSLA**	**UNH**	**AAPL**
Mean	0.00078	0.00482	0.00659	0.00066	0.00065	0.00078	0.00156	0.00168	0.00078	0.00071
St. Deviation	0.02006	0.01174	0.01672	0.01670	0.02496	0.01663	0.02716	0.03513	0.01557	0.01796
95% VaR	−0.0303	−0.0167	−0.0254	−0.0254	−0.0371	−0.0256	−0.0413	−0.0518	−0.0227	−0.0271
99% VaR	−0.0579	−0.0306	−0.0487	−0.0474	−0.0648	−0.0441	−0.0730	−0.0935	−0.0414	−0.0492
Skewness	0.02227	−0.22528	0.22318	0.18596	−0.61752	−0.24478	0.10065	−0.00501	−0.40608	−0.33763
Excess Kurtosis	6.76987	11.55336	8.06054	8.02636	24.70808	9.20387	8.41896	5.08747	14.74434	6.13944
Jarque-Bera	5,349	15,602	7,606	7,535	71,427	9,915	8,275	3021	25,449	4,452
P-value	$< 2.2e^{-16}$	$< 2.2e^{-16}$	$< 2.2e^{-16}$	$< 2.2e^{-16}$	$< 2.2e^{-16}$	$< 2.2e^{-16}$	$< 2.2e^{-16}$	$< 2.2e^{-16}$	$< 2.2e^{-16}$	$< 2.2e^{-16}$
ADF test	−14.031	−13.966	−14.385	−14.420	−13.531	−14.457	−13.796	−12.368	−15.680	−13.192
P-value	0.01	0.01	0.01	0.01	0.01	0.01	0.01	0.01	0.01	0.01
Ljung-Box	15.852	159.370	62.727	64.790	29.792	120.590	59.495	18.685	191.030	82.921
P-value	0.3225	$< 2.2e^{-16}$	$3.88e^{-8}$	$1.67e^{-8}$	0.0082	$2.2e^{-16}$	$1.44e^{-7}$	0.1773	$2.2e^{-16}$	$8.1e^{-12}$
Train Set	**AMZN**	**BRK.B**	**GOOG**	**GOOGL**	**META**	**MSFT**	**NVDA**	**TSLA**	**UNH**	**AAPL**
Mean	0.00110	0.00041	0.00069	0.00069	0.00088	0.00084	0.00151	0.00143	0.00074	0.00057
St. Deviation	0.01837	0.01138	0.01523	0.01517	0.02238	0.01586	0.02470	0.03247	0.01557	0.01704
95% VaR	−0.0262	−0.0150	−0.0220	−0.0226	−0.0312	−0.0215	−0.0329	−0.0455	−0.0219	−0.0254
99% VaR	−0.0540	−0.0337	−0.0457	−0.0460	−0.0586	−0.0415	−0.0680	−0.0885	−0.0418	−0.0482
Skewness	0.01920	−0.35895	0.40331	0.31635	0.51447	−0.33589	0.13938	0.09633	−0.74042	−0.59672
Excess Kurtosis	7.91823	16.47421	12.71639	12.91847	18.40722	14.08059	15.36306	6.98376	18.51447	8.78281
Jarque-Bera	5,347	23,235	13,814	14,233	28,919	16,907	20,088	4,153	29,352	6,684
P-value	$< 2.2e^{-16}$	$< 2.2e^{-16}$	$< 2.2e^{-16}$	$< 2.2e^{-16}$	$< 2.2e^{-16}$	$< 2.2e^{-16}$	$< 2.2e^{-16}$	$< 2.2e^{-16}$	$< 2.2e^{-16}$	$< 2.2e^{-16}$
ADF test	−13.506	−12.826	−13.877	−13.878	−13.247	−13.937	−13.974	−11.893	−15.706	−12.873
P-value	0.01	0.01	0.01	0.01	0.01	0.01	0.01	0.01	0.01	0.01
Ljung-Box	22.169	191.940	74.883	77.539	23.867	140.020	74.044	12.441	176.580	80.308
P-value	0.0752	$< 2.2e^{-16}$	$2.49e^{-10}$	$8.07e^{-11}$	0.0476	$2.2e^{-16}$	$3.54e^{-10}$	0.5709	$2.2e^{-16}$	$2.48e^{-11}$
Test Set	**AMZN**	**BRK.B**	**GOOG**	**GOOGL**	**META**	**MSFT**	**NVDA**	**TSLA**	**UNH**	**AAPL**
Mean	$-5.13e^{-5}$	$6.73e^{-4}$	$5.77e^{-4}$	$5.75e^{-4}$	$2.15e^{-5}$	$6.08e^{-4}$	$1.68e^{-3}$	$2.35e^{-3}$	$8.72e^{-4}$	$1.11e^{-3}$
St. Deviation	0.02401	0.01267	0.02021	0.02037	0.03086	0.01855	0.03288	0.04147	0.015578	0.02024
95% VaR	−0.0353	−0.0194	−0.0322	−0.0326	−0.0423	−0.0298	−0.0544	−0.0667	−0.0241	−0.0329
99% VaR	−0.0716	−0.0287	−0.0519	−0.0527	−0.0702	−0.0470	−0.0803	−0.1018	−0.0366	−0.0516
Skewness	−0.14019	0.02910	0.00752	0.03257	−1.70759	−0.07889	0.04569	−0.15445	0.49297	0.07008
Excess Kurtosis	7.46990	5.52214	5.50835	5.33549	27.73803	4.54782	3.88102	5.30186	7.57891	4.96820
Jarque-Bera	634	201	199	173	19,722	77	25	171	694	123
P-value	$< 2.2e^{-16}$	$< 2.2e^{-16}$	$< 2.2e^{-16}$	$< 2.2e^{-16}$	$< 2.2e^{-16}$	$< 2.2e^{-16}$	$4.1e^{-06}$	$< 2.2e^{-16}$	$< 2.2e^{-16}$	$< 2.2e^{-16}$
ADF test	−9.443	−8.763	−9.433	−9.566	−9.799	−9.482	−7.796	−7.856	−9.677	−9.182
P-value	0.01	0.01	0.01	0.01	0.01	0.01	0.01	0.01	0.01	0.01
Ljung-Box	11.179	8.457	21.696	22.142	15.367	30.008	13.720	12.490	20.765	14.090
P-value	0.6719	0.8642	0.0851	0.0757	0.3536	0.0076	0.4708	0.5671	0.1078	0.443

Table 4.2: Descriptive statistics of the log-returns

It can be seen from Table 4.2 that the assets do possess heavier tails than those of the normal distribution since the Jarque-Bera test rejects the null hypothesis of normally distributed data for all 10 assets in all three periods. To investigate the distribution of the assets further, the Q-Q plots of all 10 assets are shown below in Figure 4.3 for the full sample.

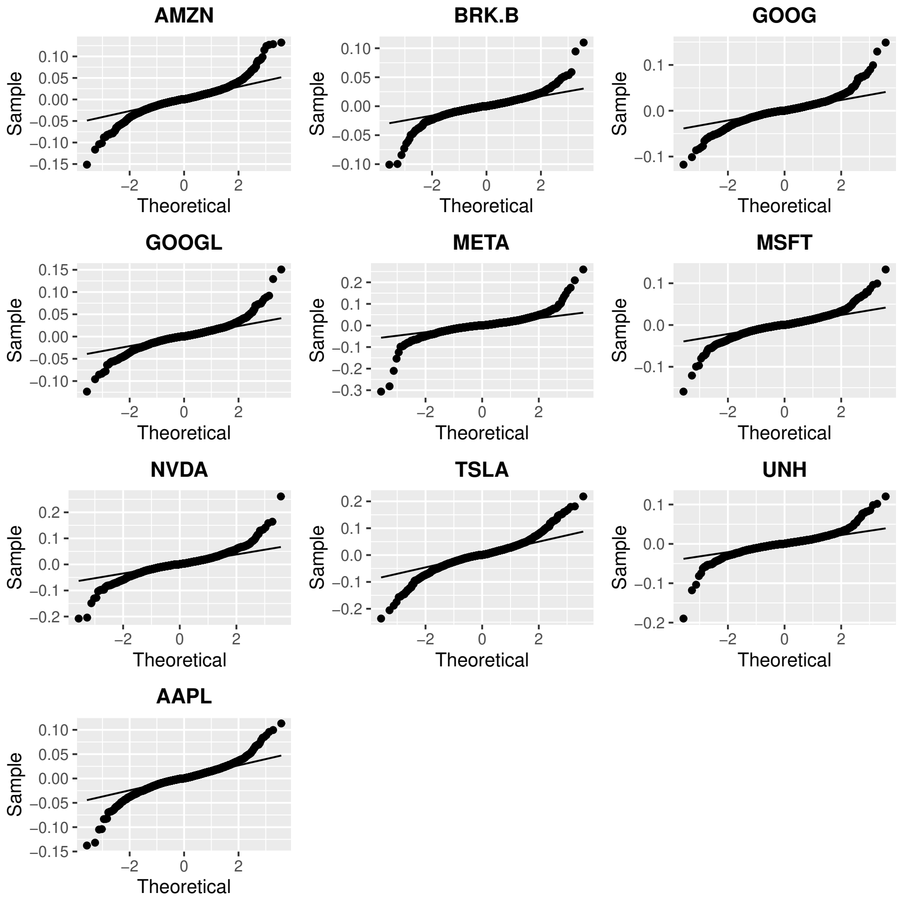

Figure 4.3: Q-Q plots based on the full sample

It can be seen from Figure 4.3 that all 10 assets have heavy tails. The upper tails are heaviest for META, NVDA and TSLA, whereas the lower tails are heaviest for META, NVDA, TSLA and UNH. Thus, a distribution should be fitted which takes these heavy tails into consideration. In this project, the ARMA-GARCH models will be used to model the marginal distributions, as they exhibit heavy tails and are a great choice when modelling volatile data [Ruppert and Matteson, 2015, page 413].

4.2 Marginal Distributions

This section is based on [Ruppert and Matteson, 2015, pp. 405-443].

In this section, the marginal distributions, from which the copulas will be constructed, are fitted. As mentioned in Chapter 1, this is done by the use of ARMA-GARCH models. The inclusion of the GARCH part is of great use in the modelling of economic and financial data, as it captures time-varying volatility, which is often more common than constant volatility. Moreover, the GARCH processes also exhibit heavy tails, which are also often seen in financial data. Moreover, the chosen data exhibit heavy tails which is seen in Figure 4.3.

An autoregressive moving average (ARMA) model consists of two parts, namely the autoregressive (AR) part and the moving average (MA) part. An ARMA(p,q) model, which is a combination of an AR(p) model and a MA(q) model, is defined below.

Definition 4.1 (ARMA Process).
$\{X_t\}$ is an ARMA(p,q) process if $\{X_t\}$ is stationary and if for every t,

$$X_t - \phi_1 X_{t-1} - \cdots - \phi_p X_{t-p} = W_t + \theta_1 W_{t-1} + \cdots + \theta_q W_{t-q},$$

or equivalently

$$\phi(B)X_t = \theta(B)W_t,$$

where $\{W_t\} \sim WN(0,\sigma^2)$, and the pth and qth degree polynomials $\phi(z) = (1 - \phi_1 z - \cdots - \phi_p z^p)$ and $\theta(z) = (1 - \theta_1 z + \cdots + \theta_q z^q)$ have no common factors.

Thus, the ARMA process depends both on lagged values of itself as well as lagged values of the noise process.

The autoregressive conditional heteroskedasticity process, ARCH, is defined as:

Definition 4.2 (ARCH Process).
The ARCH(p) process, $\{Y_t\}$ is the stationary solution of the equation

$$W_t = \sigma_t \varepsilon_t, \quad \{\varepsilon_t\} \sim IIDN(0,1), \tag{4.1}$$

where σ_t^2 is the function of $\{W_s, s < t\}$ defined by

$$\sigma_t^2 = \omega + \sum_{i=1}^{p} \alpha_i Y_{t-i}^2, \tag{4.2}$$

with $\omega > 0$ and $\alpha_1 \geq 0$ for $i = 1, \ldots, p$.

The generalized ARCH process is defined below.

Definition 4.3 (GARCH Process).
The GARCH(p, r) process is a generalization of the ARCH(p) process, in which the variance in (4.2) is replaced by

$$\sigma_t^2 = \omega + \sum_{i=1}^{p} \alpha_i Y_{t-i}^2 + \sum_{i=1}^{r} \beta_i \sigma_{t-i}^2, \tag{4.3}$$

with $\omega > 0$ and $\alpha_i, \beta_i \geq 0$ for $i = 1, 2, \ldots$.

In this project the ARMA$(0,0)$-GARCH$(1,1)$ model and ARMA$(1,1)$-GARCH$(1,1)$ model are fitted, which are given as:

$$\begin{aligned} ARMA(0,0): &\quad X_t = W_t, \\ ARMA(1,1): &\quad X_t - \phi_1 X_{t-1} = W_t + \theta_1 W_1, \end{aligned}$$

where $W_t = \sigma_t \varepsilon_t$, for $\{\varepsilon_t\} \sim IIDN(0,1)$, and $\sigma_t = \sqrt{\omega + \alpha_1 Y_{t-1}^2 + \beta_1 + \sigma_{t-1}^2}$.

The assumption of normality in (4.1) can be relaxed, and thus a general GARCH(p, r) process can be defined as a stationary process $\{Y_t\}$ satisfying (4.3) and the generalized form of (4.1),

$$Y_t = \sigma_t \varepsilon_t, \quad \{\varepsilon_t\} \sim IID(0,1).$$

However, in this project three different density functions for ε_t will be assumed; Normal, Student's t and skewed Student's t. The density function for the skewed Student's t-distribution is given by

$$f(x; \nu, \lambda) = \begin{cases} bc(1 + \frac{1}{\nu-2}(\frac{bx+a}{1-\lambda})^2)^{-(\nu+1)/2)} & \text{if } x < -a/b, \\ bc(1 + \frac{1}{\nu-2}(\frac{bx+a}{1+\lambda})^2)^{-(\nu+1)/2} & \text{if } x \geq -a/b, \end{cases}$$

where $2 < \nu < \infty$ denotes the degree of freedom and $-1 < \lambda < 1$ denotes the asymmetry parameter. The constants a, b and c are given by

$$a = 4\lambda c \left(\frac{\nu - 2}{\nu - 1} \right), \quad b = \sqrt{1 + 3\lambda^2 - a^2}, \quad \text{and} \quad c = \frac{\Gamma(\frac{\nu+1}{2})}{\sqrt{\pi(\nu-2)\Gamma(\frac{\nu}{2})}}.$$

If $\lambda = 0$ the skewed Student's t-distribution reduces to the Student's t-distribution and if both $\lambda = 0$ and $\nu \to \infty$, it reduces to the Normal density.

One of the notable features of the financial data captured by GARCH models is the persistence of volatility. Thus, large or small fluctuations in the data are often followed by fluctuations of comparable magnitude. GARCH models reflect this as they incorporate correlation in the sequence $\{\sigma_t^2\}$ of conditional variances.

Now that the ARMA-GARCH models are defined, they can be fitted on the training set. As seen in Table 4.2 all the 10 assets are stationary, as the ADF test rejects the null hypothesis for every asset. However, the Ljung-Box test showed that autocorrelation was present for most of the 10 assets in the full sample and train set, which makes it reasonable to fit an ARMA-GARCH model to the data in order to model the autocorrelation. Both an ARMA$(0,0)$-GARCH$(1,1)$ model and ARMA$(1,1)$-GARCH$(1,1)$ model are compared assuming three different marginal distributions; the Normal distribution, the t-distribution and the Skewed t-distribution. The log-likelihood (LL), Akaike's Information Criteria (AIC) and Bayes Information Criteria (BIC) for the ARMA$(0,0)$-GARCH$(1,1)$ model are shown below.

ARMA(0,0)-GARCH(1,1)										
Normally distributed standardized residuals										
	AMZN	**BRK.B**	**GOOG**	**GOOGL**	**META**	**MSFT**	**NVDA**	**TSLA**	**UNH**	**AAPL**
LL	5,145.77	6,318.49	5,548.41	5,550.37	4,794.27	5,570.06	4,642.28	4,107.42	5,702.88	5,376.00
AIC	−5.295	−6.503	−5.710	−5.712	−4.933	−5.732	−4.777	−4.226	−5.869	−5.532
BIC	−5.284	−6.492	−5.699	−5.701	−4.922	−5.721	−4.765	−4.215	−5.858	−5.521
t-distributed standardized residuals										
	AMZN	**BRK.B**	**GOOG**	**GOOGL**	**META**	**MSFT**	**NVDA**	**TSLA**	**UNH**	**AAPL**
LL	5,350.52	6,403.44	5,764.30	5,757.59	5,084.35	5,761.00	4,904.63	4,271.28	5,705.79	5,528.04
AIC	−5.505	−6.590	−5.931	−5.924	−5.231	−5.928	−5.505	−4.394	−5.977	−5.688
BIC	−5.491	−6.575	−5.917	−5.910	−5.217	−5.914	−5.032	−4.379	−5.963	−5.674
Skewed t-distributed standardized residuals										
	AMZN	**BRK.B**	**GOOG**	**GOOGL**	**META**	**MSFT**	**NVDA**	**TSLA**	**UNH**	**AAPL**
LL	5,350.97	6,403.99	5,764.44	5,757.59	5,084.39	5,761.46	4,904.79	4,271.29	5,808.84	5,528.07
AIC	−5.505	−6.589	−5.930	−5.923	−5.230	−5.927	−5.045	−4.393	−5.976	−5.687
BIC	−5.487	−6.572	−5.913	−5.906	−5.213	−5.910	−5.028	−4.376	−5.959	−5.670

Table 4.3: Model selection criteria of the ARMA(0,0)-GARCH(1,1) model

It can be seen that the model with t-distributed residuals performs best for all 10 assets both in regard to the log-likelihood, AIC, and BIC values.

The results for the ARMA$(1,1)$-GARCH$(1,1)$ model are shown below in Table 4.4.

ARMA(1,1)-GARCH(1,1)										
Normally distributed standardized residuals										
	AMZN	**BRK.B**	**GOOG**	**GOOGL**	**META**	**MSFT**	**NVDA**	**TSLA**	**UNH**	**AAPL**
LL	$5,247.30$	$6,322.36$	$5,548.98$	$5,550.99$	$4,794.36$	$5,576.44$	$4,644.01$	$4,107.46$	$5,710.06$	$5,376.03$
AIC	-5.295	-6.505	-5.709	-5.711	-4.931	-5.737	-4.777	-4.224	-5.874	-5.530
BIC	-5.278	-5.488	-5.691	-5.693	-4.914	-5.720	-4.759	-4.207	-5.857	-5.513
t-distributed standardized residuals										
	AMZN	**BRK.B**	**GOOG**	**GOOGL**	**META**	**MSFT**	**NVDA**	**TSLA**	**UNH**	**AAPL**
LL	$5,351.78$	$6,408.49$	$5,766.07$	$5,859.56$	$5,089.38$	$5,772.30$	$4,906.11$	$4,271.91$	$5,817.63$	$5,528.20$
AIC	-5.504	-6.593	-5.931	-5.924	-5.234	-5.938	-5.045	-4.392	-5.984	-5.686
BIC	-5.484	-6.573	-5.911	-5.904	-5.214	-5.917	-5.025	-4.372	-5.964	-5.666
Skewed t-distributed standardized residuals										
	AMZN	**BRK.B**	**GOOG**	**GOOGL**	**META**	**MSFT**	**NVDA**	**TSLA**	**UNH**	**AAPL**
LL	$5,352.29$	$6,408.82$	$5,766.21$	$5,759.56$	$5,089.40$	$5,772.37$	$4,906.27$	$4,271.93$	$5,817.96$	$5,528.22$
AIC	-5.504	-6.592	-5.930	-5.923	-5.233	-5.937	-5.045	-4.391	-5.984	-5.685
BIC	-5.481	-6.569	5.907	-5.900	-5.210	-5.914	-5.022	-4.368	-5.961	-5.662

Table 4.4: Model selection criteria of the ARMA(1,1)-GARCH(1,1) model

Again, it can be seen that the model with t-distributed residuals performs best for all 10 assets based on both log-likelihood, AIC and BIC. Moreover, it can be seen that the best model for MSFT and UNH is the ARMA$(1,1)$-GARCH$(1,1)$ model, whereas the ARMA$(0,0)$-GARCH$(1,1)$ model performs best for the remaining 8 assets.

To check whether it is reasonable to fit an ARMA-GARCH model, and not just an ARMA model, the heteroskedasticity of the ARMA models is checked. This is done by performing the Ljung-Box test on the squared residuals of the ARMA models. The results can be seen below in Table 4.5.

Ljung-Box test on the squared residuals of the ARMA models										
	AMZN		**BRK.B**		**GOOG**		**GOOGL**		**META**	
Lag	ARMA(0,0)		ARMA(0,0)		ARMA(0,0)		ARMA(0,0)		ARMA(0,0)	
	Q-stat.	P-value	Q-stat.	P-value	Q-stat.	P-value	Q-stat.	P-value	Q-stat.	P-value
5	73.7	$1.8e^{-14}$	2377.8	$< 2e^{-16}$	233.5	$< 2e^{-16}$	236.6	$< 2e^{-16}$	29.4	$1.9e^{-5}$
10	104.3	$< 2e^{-16}$	3231.5	$< 2e^{-16}$	294.6	$< 2e^{-16}$	301.1	$< 2e^{-16}$	35.2	$1.2e^{-4}$
15	122.1	$< 2e^{-16}$	4086.4	$< 2e^{-16}$	349.3	$< 2e^{-16}$	356.9	$< 2e^{-16}$	47.3	$3.3e^{-5}$
	MSFT		**NVDA**		**TSLA**		**UNH**		**AAPL**	
Lag	ARMA(1,1)		ARMA(0,0)		ARMA(0,0)		ARMA(1,1)		ARMA(0,0)	
	Q-stat.	P-value	Q-stat.	P-value	Q-stat.	P-value	Q-stat.	P-value	Q-stat.	P-value
5	764.6	$< 2e^{-16}$	216.2	$< 2e^{-16}$	329.0	$< 2e^{-16}$	895.4	$< 2e^{-16}$	740.4	$< 2e^{-16}$
10	912.0	$< 2e^{-16}$	265.1	$< 2e^{-16}$	392.1	$< 2e^{-16}$	1623	$< 2e^{-16}$	1011.4	$< 2e^{-16}$
15	1092.0	$< 2e^{-16}$	288.4	$< 2e^{-16}$	428.5	$< 2e^{-16}$	2047.6	$< 2e^{-16}$	1351.7	$< 2e^{-16}$

Table 4.5: Test for heteroskedasticity in the squared residuals of the ARMA models

It can be seen that the Ljung-Box test rejects the null hypothesis of no autocorrelation for both lag 5, 10 and 15 for all 10 assets. Thus, it is reasonable to assume, that ARMA-GARCH models are more appropriate to fit than pure ARMA models. Thus the best ARMA-GARCH models, evaluated based on Table 4.3 and 4.4, are fitted.

The parameter estimates and statistical tests for the marginal distributions can be seen below in Table 4.6 for AMZN, BRK.B, GOOG, GOOGL and META. Note that all assets' marginal distributions also include the GARCH$(1,1)$ part.

Parameter estimates of the marginal distributions and statistic tests - the first 5 assets										
	AMZN		**BRK.B**		**GOOG**		**GOOGL**		**META**	
	ARMA(0,0)		ARMA(0,0)		ARMA(0,0)		ARMA(0,0)		ARMA(0,0)	
	Value	P-value	Value	P-value	Value	P-value	Value	P-value	Value	P-value
μ	$1.43e^{-3}$	$1.34e^{-6}$	$5.63e^{-4}$	0.002	$9.30e^{-4}$	0.000	$9.63e^{-4}$	$7.98e^{-5}$	$1.16e^{-3}$	$2.75e^{-4}$
ϕ										
θ										
ω	$3.62e^{-5}$	$6.74e^{-5}$	$8.18e^{-6}$	0.000	$8.67e^{-6}$	0.000	$7.80e^{-6}$	0.000	$1.69e^{-6}$	0.467
α	0.156	$3.58e^{-6}$	0.107	0.000	0.058	0.000	0.053	0.000	0.027	$7.03e^{-5}$
β	0.746	0.000	0.812	0.000	0.902	0.000	0.909	0.000	0.968	0.000
ν	3.734	0.000	4.897	0.000	3.678	0.000	3.764	0.000	3.671	$4.32e^{-13}$
Ljung-Box test on the standardized residuals										
Lag	Q-stat.	P-value	Q-stat.	P-value	Q-stat.	P-value	Q-stat.	P-value	Q-stat.	P-value
5	5.379	0.371	9.366	0.095	7.746	0.171	7.792	0.168	2.245	0.814
10	8.534	0.577	16.261	0.092	18.355	0.049	17.859	0.057	4.280	0.934
15	15.102	0.444	17.809	0.273	20.706	0.147	20.186	0.165	7.420	0.945
Ljung-Box test on the squared standardized residuals										
Lag	Q-stat.	P-value	Q-stat.	P-value	Q-stat.	P-value	Q-stat.	P-value	Q-stat.	P-value
5	1.378	0.927	6.199	0.287	0.565	0.990	0.412	0.995	0.134	1
10	2.514	0.991	10.683	0.383	2.246	0.994	1.837	0.997	0.533	1
15	3.080	1	11.839	0.691	3.124	1	2.668	1	0.850	1

Table 4.6: Estimation results for the first 5 assets based on the chosen models

It can be seen in the above table, that μ is significant for all 5 assets. Moreover, μ has the highest value for AMZN, which is also seen in Table 4.2, where AMZN had the highest mean value of the five assets in the training set. Furthermore, it can be seen that both ω, α, β, and ν are significant for all five models, except ω which is not significant for META. This indicates that the proposed ARMA-GARCH models are a good choice.
In regard to the statistical tests, the Ljung-Box test has been performed on the standardized residuals to test for autocorrelation and the squared standardized residuals to test for GARCH effects. It can be seen that the null hypothesis of no autocorrelation in the standardized residuals is not rejected for either lag 5, 10, or 15 on all five assets except for lag 10 for GOOG. Moreover, the null hypothesis of no autocorrelation in the squared standardized residuals is also not rejected at either lag 5, 10, or 15 for either of the assets. These results indicate that the marginal distributions seem to be nicely fitted for all assets.

The parameter estimates and statistical tests for the marginal distributions can be seen below in Table 4.7 for MSFT, NVDA, TSLA, UNH and AAPL. Note once more, that all assets' marginal distributions also include the GARCH$(1, 1)$ part.

Parameter estimates of the marginal distributions and statistic tests - the last 5 assets										
	MSFT		**NVDA**		**TSLA**		**UNH**		**AAPL**	
	ARMA(1,1)		ARMA(0,0)		ARMA(0,0)		ARMA(1,1)		ARMA(0,0)	
	Value	P-value	Value	P-value	Value	P-value	Value	P-value	Value	P-value
μ	0.001	$12.43e^{-10}$	$1.19e^{-3}$	0.001	1.26^{-3}	0.015	$9.60e^{-4}$	$1.89e^{-11}$	1.10^{-3}	$4.88e^{-5}$
ϕ	0.820	0.000					0.909	0.000		
θ	-0.878	0.000					-0.945	0.000		
ω	0.000	0.000	$5.68e^{-6}$	0.162	0.031	$1.45e^{-10}$	$2.16e^{-6}$	0.047	$1.60e^{-5}$	0.022
α	0.111	0.000	0.033	0.000	0.956	$1.25e^{-12}$	0.047	0.110	0.108	$1.96e^{-4}$
β	0.840	0.000	0.957	0.000	0.956	0.000	0.945	0.000	0.846	0.000
ν	3.705	0.000	3.384	0.000	3.458	0.000	4.173	0.000	3.650	0.000
Ljung-Box test on the standardized residuals										
Lag	Q-stat.	P-value	Q-stat.	P-value	Q-stat.	P-value	Q-stat.	P-value	Q-stat.	P-value
5	6.948	0.225	3.871	0.568	0.216	0.999	3.964	0.555	5.02	0.413
10	12.791	0236	11.777	0.300	4.506	0.922	6.589	0.764	10.416	0.405
15	22.911	0.086	21.519	0.121	9.164	0.869	9.583	0.845	17.668	0.281
Ljung-Box test on the squared standardized residuals										
Lag	Q-stat.	P-value	Q-stat.	P-value	Q-stat.	P-value	Q-stat.	P-value	Q-stat.	P-value
5	1.359	0.929	1.720	0.886	6.291	0.279	4.329	0.503	5.128	0.400
10	3.132	0.978	2.401	0.992	12.950	0.227	9.135	0.519	7.508	0.677
15	4.636	0.995	3.363	0.999	16.156	0.372	10.817	0.766	11.015	0.752

Table 4.7: Estimation results for the last 5 assets based on the chosen models

Once again, it can be seen from the above table that μ is significant for all five assets. Moreover, the highest value of μ is found for NVDA, which also supports the findings of Table 4.2 in the training set. It can be seen that ϕ and θ are significant for both MSFT and UNH. This makes great sense as it was found from Table 4.3 and Table 4.4 that the ARMA$(1, 1,)$-GARCH$(1, 1)$ model performed better than the ARMA$(0, 0)$-GARCH$(1, 1)$ model based on both the log-likelihood, AIC, and BIC values. Additionally, it can be seen that ω is significant for all assets except NVDA and α is significant for all assets except UNH. In regard to β and ν, they were found to be significant for all five assets. This indicates that the proposed ARMA-GARCH models seem to be a great choice of models for the data.
Both the Ljung-Box test performed on the standardized residuals and the Ljung-Box test performed on the squared standardized residuals reject the null hypothesis of no autocorrelation for all five assets. Thus, the model fits of these five assets also seem reasonable.

4.3 Copulas

In this section, the Normal copula, the t-copula, and the four Archimedean copulas described in Section 2.1 are estimated based on the data. All copula models are fitted with t-distributed marginal distributions, as this was found to be the best-fitting marginal in Section 4.2. The estimated copula parameters as well as the log-likelihood, AIC and BIC values are given below.

Copula	Parameter	df	LL	AIC	BIC
Normal	0.7206		$5,714$	$-11,426$	$-11,420$
Student's t	0.5075	4	$5,949$	$-11,894$	$-11,883$
Clayton	1.106		$4,303$	$-8,604$	$-8,598$
Gumbel	1.863		$5,240$	$-10,478$	$-10,473$
Frank	4.874		$5,067$	$-10,131$	$-10,125$
Joe	2.346		$4,549$	$-9,096$	$-9,091$

Table 4.8: Results from fitting copulas

It can be seen that the Student's t-copula is preferred based on log-likelihood, AIC and BIC value. The second best copula is the Normal copula followed by the Gumbel copula and the Frank copula. The worst-fitting copula is the Clayton copula followed by the Joe copula.

To investigate how well the fitted copulas represent the actual data in regards to distribution and tail dependency, log-returns have been computed based on $2,042$ simulated values of both the Student's t-copula, Normal copula, Gumbel copula, and Frank copula. To visualize the fit of the simulated and observed values, the simulated and observed log-returns of the pair AMZN & BRK.B are observed below.

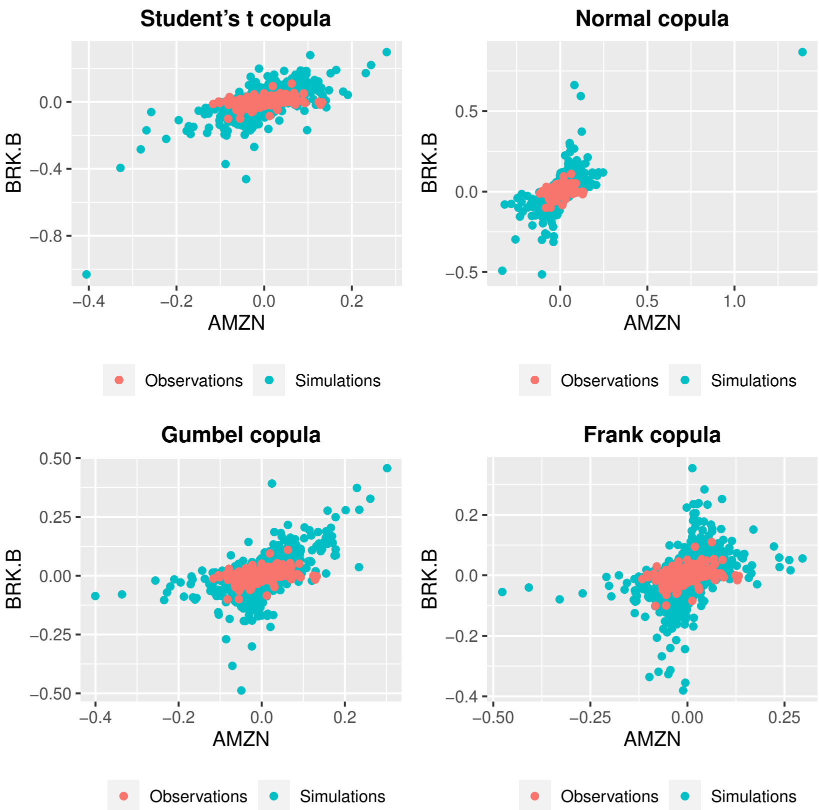

Figure 4.4: Observed vs. simulated log-returns for AMZN and BRK.B from 2nd of June 2012 until 31st of March 2020

It can be seen from the plots, that even though the results from Table 4.8 indicated that a t-copula was the best fit of the proposed copulas, it is not fitting well. The biggest concern is in regards to the tail dependency, where the t-copula assigns way more weight to the tails than the data indicates. The observed log-returns do have weight in the tails, however not as much as the t-copula assumes. Nevertheless, it is seen that the simulated log-returns from the t-copula, despite having too heavy tails, still resemble the data better than the other proposed copulas.

4.4 Value-at-Risk Forecast

In this section, one-day-ahead out-of-sample VaR is forecasted using the procedure described in Section 3.3. In the procedure, $N = 10.000$ Monte Carlo simulations and $M = 759$ one-day-ahead out-of-sample forecasts are used. The obtained VaR forecasts are evaluated using the described backtesting methods from Section 3.4, both in regard to the statistical tests and the loss functions.

In the following table, the forecasting performance of the procedure can be seen based on the four best-fitting copulas found in Table 4.8 with t-distributed standardized residuals. Both the ratio of VaR exceedances, Z/T, Kupiec's unconditional coverage test, LR_{UC} and Christoffersen's independence test, LR_{CC}, are given for the 95% and 99% VaR.

	95% VaR			99% VaR		
Copula	Z/T	LR_{UC}	LR_{CC}	Z/T	LR_{UC}	LR_{CC}
Normal	0.01054	43.161	43.257	0	15.256	15.256
P-value		$5.04e^{-11}$	$4.04e^{-10}$		$9.39e^{-5}$	$4.87e^{-4}$
Student's t	0.00791	36.218	36.389	0	15.256	15.256
P-value		$1.76e^{-9}$	$1.25e^{-8}$		$9.39e^{-5}$	$4.87e^{-4}$
Gumbel	0.01728	22.899	23.353	0	15.256	15.256
P-value		$1.71e^{-6}$	$8.49e^{-6}$		$9.39e^{-5}$	$4.87e^{-4}$
Frank	0.01581	25.190	25.576	0.00395	3.638	3.662
P-value		$5.19e^{-7}$	$2.79e^{-6}$		0.056	0.160

Table 4.9: Value-at-Risk forecast performance

The table shows an overall bad performance of all four copulas for both the 95% VaR and 99% VaR, as the tests result in values way lower than the proposed 0.05 and 0.01 levels. However, it can be seen that the Gumbel copula is closest to the desired ratio of VaR exceedances for the 95% VaR, whereas the Frank copula is closest for the 99% VaR. Nevertheless, the results do not coincide with the ones found in Table 4.8 in which the t-copula was found to perform best. In regards to the likelihood ratio tests, the Frank copula for the 99% VaR is the only one for which the null hypothesis is not rejected. Thus, the backtesting analysis indicates that the Frank copula is the preferred copula for modelling the assets of the portfolio.

Next, the loss functions given in Section 3.4 are used to determine which copula performs best. Both backtesting based on the loss function provided by Lopez, $\hat{C}^L$, and backtesting based on the loss function provided by Blanco and Ihle, $\hat{C}^{BI}$, is performed. The results of the loss functions for the 95% VaR are shown below.

	95% VaR	
Copula	$\hat{C}^L$	$\hat{C}^{BI}$
Normal	0.03341	0.00165
Student's t	0.03891	0.00178
Gumbel	0.14476	0.00326
Frank	0.06844	0.00315

Table 4.10: Loss functions

It can be seen from the table, that the lowest value of both $\hat{C}^L$ and $\hat{C}^{BI}$ is found for the Normal copula. Note that only the 95% VaR is evaluated, as it was found in Table 4.9 that the 99% VaR resulted in Z/T being 0 for three out of the four tested copulas.

To illustrate the predictive performance of the VaR, the portfolio returns as well as the 95% VaR, and 99% VaR, are plotted in Figure 4.5. The figure shows the forecasts based on the Monte Carlo procedure for the Normal copula, Gumbel copula and Frank copula. The Normal copula is plotted as this resulted in the lowest $\hat{C}^L$ and $\hat{C}^{BI}$ for the 95% VaR, whereas the Gumbel and Frank copulas provided the best results of Z/T for the 95% VaR and 99% VaR, respectively.

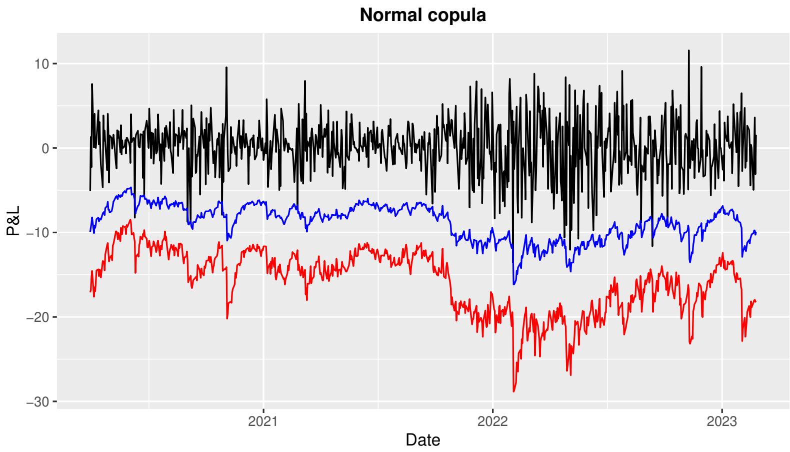

(a) Forecast performance with the Normal copula

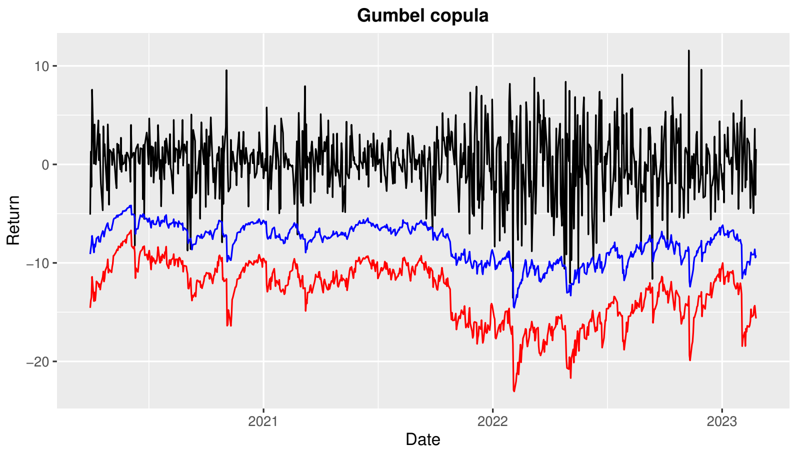

(b) Forecast performance with the Gumbel copula

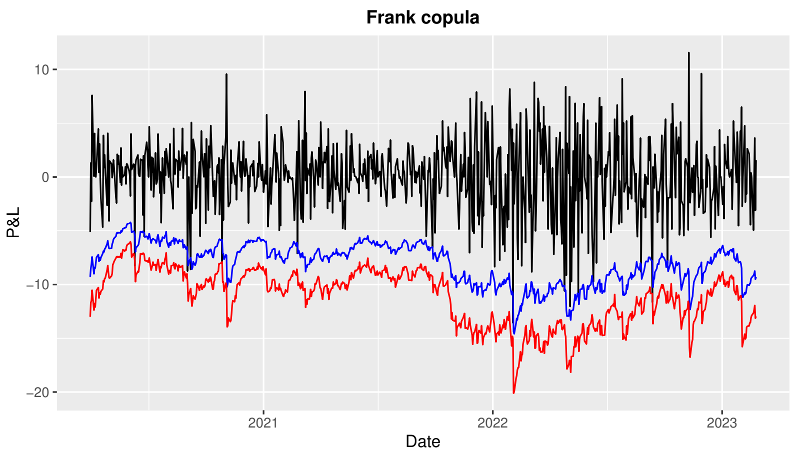

(c) Forecast performance with the Frank copula

Figure 4.5: Visualization of the P&L function with the obtained VaR forecasts from the Monte Carlo procedure. The blue curve represents the 95% VaR and the red curve represents the 99% VaR.

5 Further Analysis of Value-at-Risk

In this chapter further analysis of the Value-at-Risk will be conducted. This first implies an analysis of the previously noted train and test sets, to analyze whether the Value-at-Risk performance is better in these subperiods than in the full period. Afterwards, the Value-at-Risk performance of the portfolio will be compared with the Value-at-Risk performance of the S&P500 index. This is done in order to investigate whether the portfolio is representative of the index in regard to risk estimation.

5.1 Train and Test Set

In this section, the VaR will be estimated for the portfolio for the previously specified train and test periods. First, the train set, from now on denoted the original train set, will be observed, which includes daily observations from the 1st of June 2012 until the 31st of March 2020. Afterwards, the test set, from now on denoted the original test set, will be observed, which includes daily observations in the period from the 1st of April 2020 until the 27th of February 2023. This decision has been made, as Figure 4.1 shows a significant difference in the prices in the two periods, and it is possible that the forecasting performance found in Section 4.4 suffered from this. However, the same procedure will take place, thus firstly the data will be analyzed, then marginal distributions will be fitted, next the best-fitting copula will be determined and lastly the Value-at-Risk will be forecasted and evaluated based on the proposed Monte Carlo procedure, and backtesting techniques.

Train Set

In this subsection, the original train set will be assumed to be the full period. Moreover, a new training and test period will be determined. Thus, the full period is now from the 1st of June 2012 until the 31st of March 2020 consisting of $2,043$ days, whereas the training set consists of $1,565$ observations, corresponding to daily data from the 1st of June 2012 until the 31st of May 2018, and the test set consists of 477 observations, corresponding to daily data from the 1st of June 2018 until the

31st of March 2020. In the rest of this subsection, whenever a train set or test set is mentioned, these new subperiods are referred to.
The prices of the portfolio in the period from the 1st of June 2012 until the 31st of March 2020 can be seen below, with the dotted line responding to the division between the train and test set:

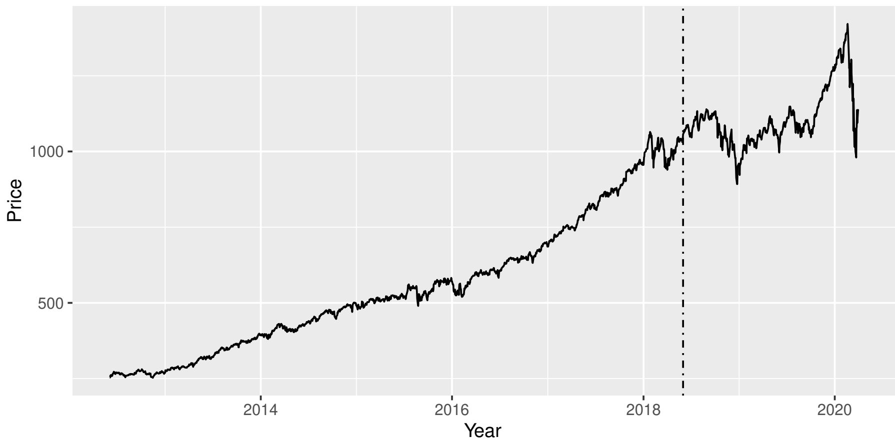

Figure 5.1: Portfolio prices from 1st of June 2012 until 31th of March 2020. The dotted line represents the division between the train and test set.

It can be seen that the prices are increasing throughout the training period, whereas they are relatively stationary in most of the test period. However, a huge spike is observed at the end of the test period. Nevertheless, the increase in the prices is not as large as in the original full period seen in Figure 4.1.

The daily prices are again transformed to log-returns to ensure stationarity. The plots of the log-returns can be seen in Figure A.1. It can be seen that the volatility is still at the same level as for the original full sample. However, the most obvious volatility clustering is not present as it takes place in the original test set. Nevertheless, it can be seen that the biggest volatility spikes, influenced by the corona pandemic, are present at the very end of the original train set for all 10 assets.

To further investigate the log-returns in the train and test periods, the descriptive statistics for these new subperiods are given in Table A.1. Note that the original train set now acts as the full sample, thus these values are not given. However, they can be seen in Table 4.2.
In regards to the mean and standard deviation, they are again almost 0 in both periods for all 10 assets. The historical 95% and 99% VaR values are all negative. For both the train and test set, the lowest values are seen for TSLA, whereas the highest values are seen for BRK.B. This coincides with the results found in Table 4.2. It can again be seen, that both right-skewed and left-skewed data are present. NVDA is the most skewed asset in the train set, whereas META is the most skewed asset

in the test set. Note that NVDA is right skewed whereas META is left skewed. This behaviour is supported by the excess kurtosis. The Jarque-Bera test rejects the null hypothesis of normally distributed log-returns for all 10 assets in both periods. Moreover, the ADF test rejects the null hypothesis of a unit root for all 10 assets in both periods. The Ljung-Box test fails to reject the null hypothesis of independently distributed observations for AMZN, META, TSLA, UNH and AAPL in the train set, whereas it only rejects the null hypothesis for TSLA in the test set.

To investigate the distribution of the assets further, the Q-Q plots of the assets are plotted in Figure A.2. It can be seen that all 10 assets have tails on approximately the same level as seen for the full sample in Figure 4.3. This motivates the choice of modelling the marginal distributions as ARMA-GARCH models.

Marginal Distibutions

As for the original full sample, it is again tested whether the marginal distributions should be modelled as an ARMA$(0, 0)$-GARCH$(0, 0)$ model or an ARMA$(1, 1)$-GARCH$(1, 1)$ model with the assumption of either normally distributed, t-distributed or skewed t-distributed standardized residuals. This resolves in the following log-likelihood, AIC and BIC values for the ARMA$(0, 0)$-GARCH$(1, 1)$ model:

ARMA(0,0)-GARCH(1,1) - Train set										
Normally distributed standardized residuals										
	AMZN	**BRK.B**	**GOOG**	**GOOGL**	**META**	**MSFT**	**NVDA**	**TSLA**	**UNH**	**AAPL**
LL	$3,844.46$	$4,900.90$	$4,300.28$	$4,296.27$	$3,676.80$	$4,231.97$	$3,614.35$	$3,183.51$	$4,384.41$	$4,104.72$
AIC	-5.243	-6.685	-5.865	-5.860	-5.014	-5.772	-4.929	-4.341	-5.980	-5.598
BIC	-5.229	-6.671	-5.851	-5.845	-5.000	-5.758	-4.914	-4.326	-5.966	-5.584
t-distributed standardized residuals										
	AMZN	**BRK.B**	**GOOG**	**GOOGL**	**META**	**MSFT**	**NVDA**	**TSLA**	**UNH**	**AAPL**
LL	$4,071.22$	$4,928.59$	$4,442.85$	$4,439.23$	$3,865.16$	$4,417.77$	$3,842.21$	$3,288.17$	$4,456.98$	$4,231.56$
AIC	-5.551	-6.722	-6.059	-6.054	-5.270	-6.024	-5.239	-4.482	-6.078	-5.770
BIC	-5.533	-6.704	-6.040	-6.036	-5.252	-6.006	-5.221	-4.464	-6.060	-5.752
Skewed t-distributed standardized residuals										
	AMZN	**BRK.B**	**GOOG**	**GOOGL**	**META**	**MSFT**	**NVDA**	**TSLA**	**UNH**	**AAPL**
LL	$4,073.26$	$4,930.00$	$4,443.58$	$4,439.54$	$3,865.41$	$4,419.94$	$3,842.29$	$3,288.17$	$4,457.03$	$4,231.79$
AIC	-5.553	-6.722	-6.058	-6.053	-5.269	-6.026	-5.237	-4.481	-6.077	-5.769
BIC	-5.531	-6.701	-6.037	-6.031	-5.247	-6.004	-5.216	-4.459	-6.055	-5.747

Table 5.1: Model selection criteria of the ARMA(0,0)-GARCH(1,1) model - Train set

It can be seen that the ARMA$(0, 0)$-GARCH$(1, 1)$ model with skewed t-distributed standardized residuals perform the best for all 10 assets in regards to the log-likelihood and AIC values. However, the BIC values show that the model with t-distributed standardized residuals results in the best model fit. The model selection is based on the BIC values, thus the ARMA$(0, 0)$-GARCH$(1, 1)$ model with t-distributed standardized residuals is chosen as the best-fitting model.

The results for the ARMA$(1, 1)$-GARCH$(1, 1)$ model can be seen below:

ARMA(1,1)-GARCH(1,1) - Train set										
Normally distributed standardized residuals										
	AMZN	**BRK.B**	**GOOG**	**GOOGL**	**META**	**MSFT**	**NVDA**	**TSLA**	**UNH**	**AAPL**
LL	$3,845.18$	$4,905.21$	$4,300.68$	$4,296.59$	$3,677.18$	$4,235.72$	$3,615.92$	$3,183.64$	$4,390.29$	$4,105.15$
AIC	-5.241	-6.688	-5.863	-5.858	-5.012	-5.774	-4.928	-4.338	-5.985	-5.696
BIC	-5.220	-6.667	-5.841	-5.836	-4.990	-5.753	-4.907	-4.316	-5.964	-5.575
t-distributed standardized residuals										
	AMZN	**BRK.B**	**GOOG**	**GOOGL**	**META**	**MSFT**	**NVDA**	**TSLA**	**UNH**	**AAPL**
LL	$4,073.23$	$4,934.53$	$4,444.42$	$4,440.92$	$3,868.32$	$4,419.38$	$3,842.82$	$3,289.01$	$4,463.79$	$4,232.30$
AIC	-5.551	-6.727	-6.058	-6.053	-5.271	-6.024	-5.237	-4.481	-6.084	-5.768
BIC	-5.526	-6.702	-6.033	-6.028	-5.246	-5.998	-5.211	-4.455	-6.059	-5.743
Skewed t-distributed standardized residuals										
	AMZN	**BRK.B**	**GOOG**	**GOOGL**	**META**	**MSFT**	**NVDA**	**TSLA**	**UNH**	**AAPL**
LL	$4,075.50$	$4,935.41$	$4,445.00$	$4,441.27$	$3,868.53$	$4,421.42$	$3,842.91$	$3,289.02$	$4,463.80$	$4,232.54$
AIC	-5.553	-6.727	-6.057	-6.052	-5.270	-6.025	-5.235	-4.479	-6.083	-5.767
BIC	-5.524	-6.698	-6.029	-6.023	-5.242	-5.996	-5.207	-4.450	-6.054	-5.738

Table 5.2: Model selection criteria of the ARMA(1,1)-GARCH(1,1) model - Train set

It can be seen from the above table that the ARMA$(1,1)$-GARCH$(1,1)$ model with skewed t-distributed standardized residuals performs best in regards to the log-likelihood and AIC value for all 10 assets. However, the BIC value indicated that the model with t-distributed standardized residuals results in the best model fit. When comparing Table 5.1 and Table 5.2 it can be seen that the ARMA$(0,0)$-GARCH$(1,1)$ model with t-distributed standardized residuals performs best in regards to the BIC value. Since the model choice is based on the BIC value, this model is chosen as the best-fitting marginal.

To check whether it is reasonable to include the GARCH part in the ARMA-GARCH model, the heteroskedasticity of the ARMA models is checked by performing the Ljung-Box test on the squared residuals of the ARMA models. The results can be seen in Table A.2. The table shows that the Ljung-Box test rejects the null hypothesis of no autocorrelation for lag 5, 10, and 15 for AMZN, BRK.B, META, TSLA, UNH and AAPL. However, for MSFT it only rejects for lag 5 and 10, for GOOG and NVDA it only rejects for lag 5, and for GOOGL it fails to reject the null hypothesis for any of the tested lags. Thus, GARCH effect is not present for GOOGL. However, for the purpose of the project, it will be assumed that GARCH effect is present for all 10 assets.

The parameter estimates and statistical tests of the fitted marginal distributions can be seen in Table A.3 for AMZN, BRK.B, GOOG, GOOGL and META, and in Table A.4 for MSFT, NVDA, TSLA, UNH and AAPL. It can be seen from the tables, that μ is significant for all 10 assets, with the value being 0.001 for all assets. Moreover, it can be seen that α, β and ν are significant for all assets, whereas ω is only significant for AMZN, BRK.B, NVDA and TSLA. This indicates that the proposed ARMA-GARCH models are a reasonable choice. In regards to the statistical tests, it can be seen that the Ljung-Box test fails to reject the null hypothesis for lag 5, 10 and 15 of both the standardized residuals and the squared standardized residuals. This again indicates that the marginal distributions seem to be nicely fitted for all 10 assets.

Copulas

Next, the Normal copula, t-copula and the four proposed Archimedean copulas are estimated based on the data. Again, all the models are fitted with t-distributed marginal distributions, as it was found in Table 5.1 that this was the best-fitting marginal. The parameter estimates, log-likelihood, AIC and BIC values are given below.

Copula	Parameter	df	LL	AIC	BIC
Normal	0.6451		2,854	−5,706.42	−5,701.13
Student's t	0.6516	6.45	3,312	−6,619.27	−6,608.69
Clayton	0.8054		2,066	−4,130.26	−4,124.97
Gumbel	1.673		2,660	−5,318.33	−5,313.04
Frank	4.125		2,619	−5,236.58	−5,231.29
Joe	2.045		2,233	−4,464.24	−4,458.95

Table 5.3: Results from fitting copulas - Train set

It can be seen that the Student's t-copula is preferred based on both log-likelihood, AIC and BIC. The second best copula is the Normal copula followed by the Gumbel copula and the Frank copula. The worst-fitting copula is the Clayton copula followed by the Joe copula.

To investigate how well the fitted copulas of the train set represent the actual data, log-returns have been calculated based on 1,565 simulated values of both the Student's t-copula, Normal copula, Gumbel copula, and Frank copula. The plots of the simulated and observed log-returns for the pair AMZN & BRK.B are seen below.

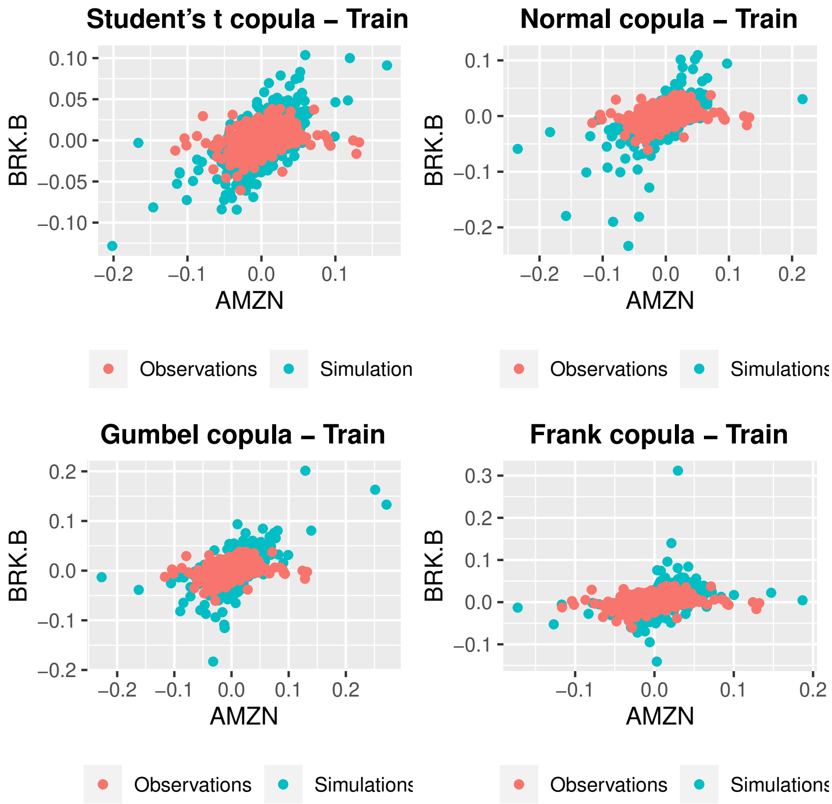

Figure 5.2: Observed vs. simulated log-returns for AMZN and BRK.B in the period from 2nd of June 2012 until 31st of May 2018

It can be seen from the plots, that the t-copula provides the best fit as indicated by Table 5.3, however, the simulated values still possess heavier tails than the actual data. Moreover, the simulated values for all of the copulas do resemble the actual data better than in the case of the original full sample seen in Figure 4.4.

Value-at-Risk Forecast

Next, one-day-ahead out-of-sample VaR is forecasted using the procedure described in Section 3.3. Again, $N = 10,000$ is chosen and $M = 477$ one-day-ahead out-of-sample forecasts are used. Once more, the obtained VaR forecasts are evaluated using the backtesting methods described in Section 3.4. The forecasting performance of the procedure can be seen below based on the four best-fitting copulas found in Table 5.3.

	95% VaR			99% VaR		
Copula	Z/T	LR_{UC}	LR_{CC}	Z/T	LR_{UC}	LR_{CC}
Normal	0.02306	9.03544	9.55591	0.00210	4.44533	4.44954
P-value		0.00265	0.00841		0.03500	0.10809
Student's t	0.02096	10.73508	11.16430	0.00210	4.44533	4.44954
P-value		0.00105	0.00376		0.03500	0.10809
Gumbel	0.03354	3.06095	4.17422	0.00839	0.13284	0.20064
P-value		0.08019	0.12405		0.71551	0.90455
Frank	0.03564	2.29162	3.55117	0.01048	0.01103	0.11719
P-value		0.13007	0.16938		0.91636	0.94309

Table 5.4: Value-at-Risk forecast performance - Train set

The table shows that the Frank copula is closest to the desired ratio of VaR exceedances for both the 95% and 99% VaR. Moreover, it can be seen that Kupiec's unconditional coverage test rejects the null hypothesis of Z/T being equal to the desired ratio of exceedances for the Normal copula and t-copula for both the 95% and 99% VaR. On the contrary, Christoffersen's independence test only rejects the null hypothesis for the Normal copula and t-copula for the 95% VaR. Again, this does not coincide with the results seen in Table 5.3.

Next, the loss functions given in Section 3.4 are used to determine which copula performs best. Both the loss function provided by Lopez and the loss function provided by Blianco and Ihle are used. The results of the loss functions for the 95% and 99% VaR are shown below.

	95% VaR		99% VaR	
Copula	$\hat{C}^L$	$\hat{C}^{BI}$	$\hat{C}^L$	$\hat{C}^{BI}$
Normal	0.08338	0.00728	0.00259	0.00023
Student's t	0.07747	0.00711	0.00236	0.00016
Gumbel	0.12919	0.01150	0.01284	0.00121
Frank	0.13437	0.01107	0.02206	0.00235

Table 5.5: Loss functions - Train set

It can be seen from the table that the lowest value of $\hat{C}^L$ and $\hat{C}^{BI}$ are found for the t-copula for both the 95% VaR and the 99% VaR.

To illustrate the predictive performance of the VaR, the portfolio returns as well as the 95% VaR, and 99% VaR, are plotted in Figure 5.3. The figure shows the forecasts based on the Monte Carlo procedure for the t-copula and Frank copula.

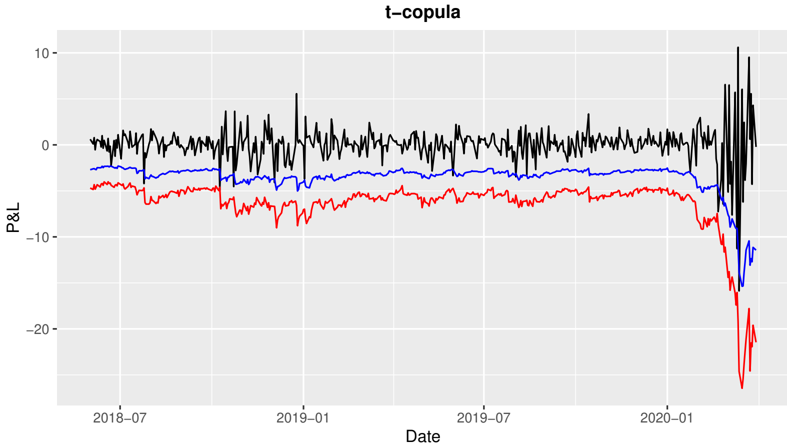

(a) Forecast performance with the t-copula

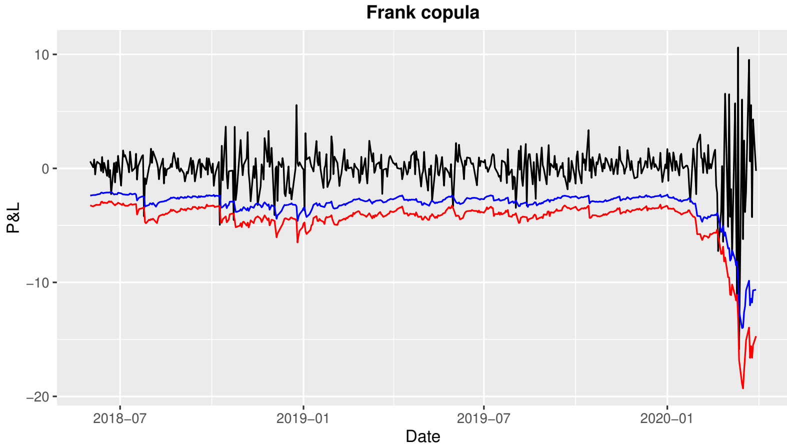

(b) Forecast performance with the Frank copula

Figure 5.3: Visualization of the P&L function with the obtained VaR forecasts from the Monte Carlo procedure. The blue curve represents the 95% VaR and the red curve represents the 99% VaR.

Test Set

In this subsection, the original test period will be assumed to be the full period. Moreover, a new training and test period will be determined. Thus, the full period is now from the 1st of April 2020 until the 27th of February 2023 consisting of 759 days, whereas the training set consists of 565 observations, corresponding to daily data from the 1st of April 2020 until the 31st of May 2022, and the test set consists of 194 observations corresponding to daily data from the 1st of June 2022 until the 27th of February 2023. The prices of the portfolio can be seen below, with the dotted line denoting the division between the new train and test set:

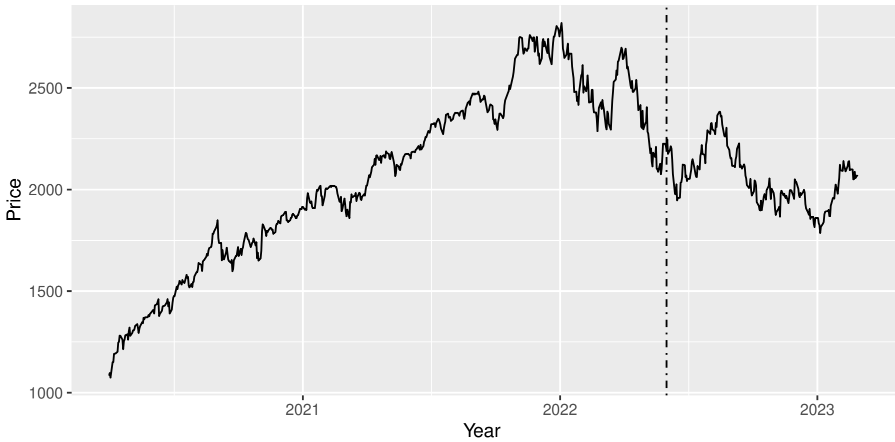

Figure 5.4: Portfolio prices from 1st of April 2020 until 27th of March 2023. The dotted line represents the division between the train and test set.

It can be seen that the prices are increasing through most of the training period before they decrease at the end of the training period. For the test period, the prices are relatively stationary but very volatile. The period from 2022 and onwards is the most volatile of the full period, which is seen in Figure 4.1.

The daily prices are again transformed to log-returns to ensure stationarity. The plots of the log-returns can be seen in Figure A.3. It can be seen that the plots are less volatile than the original full sample seen in Figure 4.2 and the original train set seen in Figure A.1. This indicates that the most volatility is present around 2020 as a result of the corona pandemic. However, there is a lot of volatility clustering in the last part of the test set, which is not seen in the previous periods.

To investigate the log-returns in the new train and test periods in more detail, the descriptive statistics for these subperiods are given in Table A.5. Note that the original test set acts as the full sample in this case. Since the descriptive statistics of these are given in Table 4.2, these are not given again.
In regards to the mean and standard deviation, they are approximately 0 for all 10 assets in both periods. The historical 95% and 99% VaR values are all negative. For both the train and test set, the lowest values are seen for TSLA, whereas the highest values are seen for BRK.B. This corresponds to the results found in Table 4.2. Once more, it can be seen that both left-skewed and right-skewed data is present. The skewness and excess kurtosis tests show that META is the most skewed asset in both the train and test periods. The Jarque-Bera test rejects the null hypothesis for all 10 assets in both periods except for TSLA in the test period. Once more, the ADF test rejects the null hypothesis of a unit root for all 10 assets in both periods. The Ljung-Box test rejects the null hypothesis of independently distributed observations for GOOG, GOOGL, and MSFT in the train set, but fails to reject the null hypothesis

for all 10 assets in the test set.

To investigate the distribution of the assets further, the Q-Q plots of the assets are plotted in Figure A.4. It can be seen that the assets have lighter tails than those of the original full sample and the original train set, as seen in Figure 4.3 and Figure A.2. However, some heavy outliers are still seen in the lower tails.

Marginal Distributions

As for the original full sample, it is again tested whether the marginal distributions should be modelled as an ARMA$(0, 0)$-GARCH$(0, 0)$ or an ARMA$(1, 1)$-GARCH$(1, 1)$ with the assumption of either normally distributed, t-distributed or skewed t-distributed standardized residuals. This resolves in the following log-likelihood, AIC and BIC values for the ARMA$(0, 0)$-GARCH$(1, 1)$ model:

ARMA(0,0)-GARCH(1,1) - Test Set										
Normally distributed standardized residuals										
	AMZN	**BRK.B**	**GOOG**	**GOOGL**	**META**	**MSFT**	**NVDA**	**TSLA**	**UNH**	**AAPL**
LL	$1,207.78$	$1,420.19$	$1,252.82$	$1,245.62$	$1,136.33$	$1,277.83$	$1,014.90$	855.44	$1,296.11$	$1,196.62$
AIC	-5.178	-6.091	-5.371	-5.340	-4.870	-5.479	-4.348	-3.662	-5.558	-5.130
BIC	-5.142	-6.055	-5.336	-5.305	-4.835	-5.443	-4.312	-3.627	-5.522	-5.094
t-distributed standardized residuals										
	AMZN	**BRK.B**	**GOOG**	**GOOGL**	**META**	**MSFT**	**NVDA**	**TSLA**	**UNH**	**AAPL**
LL	$1,225.63$	$1,430.25$	$1,281.29$	$1,271.97$	$1,151.97$	$1,290.01$	$1,022.39$	875.67	$1,321.20$	$1,210.45$
AIC	-5.250	-6.130	-5.489	-5.449	-4.933	-5.527	-4.376	-3.745	-5.661	-5.185
BIC	-5.206	-6.086	-5.445	-5.405	-4.889	-5.482	-4.331	-3.700	-5.617	-5.140
Skewed t-distributed standardized residuals										
	AMZN	**BRK.B**	**GOOG**	**GOOGL**	**META**	**MSFT**	**NVDA**	**TSLA**	**UNH**	**AAPL**
LL	$1,225.67$	$1,430.32$	$1,282.55$	$1,272.65$	$1,151.98$	$1,290.05$	$1,022.39$	876.64	$1,321.23$	$1,210.45$
AIC	-5.246	-6.126	-5.491	-5.448	-4.929	-5.523	-4.372	-3.745	-5.657	-5.180
BIC	-5.193	-6.073	-5.437	-5.395	-4.876	-5.469	-4.318	-3.691	-5.604	-5.127

Table 5.6: Model selection criteria of the ARMA(0,0)-GARCH(1,1) model - Test set

It can be seen that the ARMA$(0, 0)$-GARCH$(1, 1)$ model with t-distributed standardized residuals performs the best for all 10 assets. However, the model fit with the assumption of t-distributed standardized residuals is only slightly better than the assumption of skewed t-distributed residuals.

Below, the model selection criteria for the ARMA$(1, 1)$-GARCH$(1, 1)$ are presented.

ARMA(1,1)-GARCH(1,1) - Test Set										
Normally distributed standardized residuals										
	AMZN	**BRK.B**	**GOOG**	**GOOGL**	**META**	**MSFT**	**NVDA**	**TSLA**	**UNH**	**AAPL**
LL	$1,208.51$	$1,421.38$	$1,255.37$	$1,247.96$	$1,138.70$	$1,279.56$	$1,017.87$	855.95	$1,296.26$	$1,198.42$
AIC	-5.172	-6.088	-5.374	-5.342	-4.872	-5.478	-4.352	-3.656	-5.550	-5.129
BIC	-5.119	-6.034	-5.320	-5.288	-4.818	-5.424	-4.299	-3.602	-5.497	-5.085
t-distributed standardized residuals										
	AMZN	**BRK.B**	**GOOG**	**GOOGL**	**META**	**MSFT**	**NVDA**	**TSLA**	**UNH**	**AAPL**
LL	$1,225.63$	$1,431.25$	$1,283.54$	$1,276.26$	$1,156.07$	$1,292.87$	$1,024.75$	876.58	$1,321.57$	$1,212.53$
AIC	-5.241	-6.126	-5.491	-5.459	-4.942	-5.531	-4.377	-3.740	-5.654	-5.185
BIC	-5.179	-6.063	-5.429	-5.397	-4.880	-5.468	-4.315	-3.678	-5.592	-5.123
Skewed t-distributed standardized residuals										
	AMZN	**BRK.B**	**GOOG**	**GOOGL**	**META**	**MSFT**	**NVDA**	**TSLA**	**UNH**	**AAPL**
LL	$1,225.68$	$1,431.28$	$1,285.01$	$1,278.13$	$1,156.08$	$1,293.03$	$1,024.81$	877.37	$1,321.62$	$1,212.56$
AIC	-5.237	-6.122	-5.493	-5.463	-4.938	-5.527	-4.373	-3.739	-5.650	-5.181
BIC	-5.166	-6.050	-5.421	-5.392	-4.867	-5.456	-4.302	-3.668	-5.579	-5.110

Table 5.7: Model selection criteria of the ARMA(1,1)-GARCH(1,1) model - Test set

The above table indicates, that the ARMA$(1,1)$-GARCH$(1,1)$ model with skewed t-distributed standardized residuals results in both the highest log-likelihood and lowest AIC and BIC values for all 10 assets. However, when comparing the model selection criteria of Table 5.6 and Table 5.7 different results are seen depending on whether the log-likelihood, AIC or BIC is observed. Based on the log-likelihood, the ARMA$(1,1)$-GARCH$(1,1)$ model with skewed t-distributed standardized residuals results in the best model fit, however for the BIC value the ARMA$(0,0)$-GARCH$(1,1)$ model with t-distributed standardized residuals results in the lowest values. For the AIC value, the ARMA$(0,0)$-GARCH$(1,1)$ model with t-distributed standardized residuals results in the best model fit for all assets except GOOGL and META. Nevertheless, the model choice will be based on the BIC value, thus the ARMA$(0,0)$-GARCH$(1,1)$ model with t-distributed standardized residuals is chosen as the marginal distribution for all 10 assets.

To check whether the inclusion of the GARCH part in the ARMA-GARCH models is reasonable, the heteroskedasticity of the ARMA models is checked in Table A.6. It can be seen from the table that the Ljung-Box test rejects the null hypothesis of no autocorrelation for both lag 5, 10 and 15 for all assets except META. For META the test fails to reject the null hypothesis for all three lags. Thus, GARCH effect is not present for META, which is also seen in Figure A.3. Nevertheless, for the purpose of the project, it will again be assumed that GARCH effect is present for all 10 assets.

In Table A.7 the parameter estimates and statistical tests of the fitted marginal distributions can be seen for AMZN, BRK.B, GOOG, GOOGL, and META. Table A.8 shows the results for MSFT, NVDA, TSLA, UNH, and AAPL. It can be seen from the tables that μ is significant for all assets except AMZN, META and UNH with values between 0.001 and 0.003. Moreover, ω is significant for BRK.B, MSFT and UNH, and α is significant for all assets except GOOG and GOOGL. Lastly, β and ν are significant for all 10 assets.

Copulas

Next, the Normal copula, t-copula as well as the four proposed Archimedean copulas are estimated based on the data. Again, all the models are fitted with t-distributed marginal, since it was found in Table 5.6 that this was the best-fitting marginal. The parameter estimates as well as the log-likelihood, AIC and BIC values are given below.

Copula	Parameter	df	LL	AIC	BIC
Normal	0.6399		$1,038$	$-2,073.81$	$-2,069.67$
Student's t	0.6331	5.45	$1,187$	$-2,369.17$	$-2,360.89$
Clayton	0.9631		929.3	$-1,856.69$	$-1,852.55$
Gumbel	1.675		968.8	$-1,935.60$	$-1,931.45$
Frank	4.196		970.4	$-1,938.76$	$-1,934.62$
Joe	2		755.9	$-1,509.84$	$-1,505.70$

Table 5.8: Results from fitting copulas

It can be seen that the Student's t-copula is preferred based on both log-likelihood, AIC and BIC. The second best copula is the Normal copula followed by the Frank copula and the Gumbel copula. The worst-fitting copula is the Joe copula followed by the Clayton copula.

To investigate how well the fitted copulas represent the actual data, log-returns have been calculated based on 565 simulated values of both the Student's t-copula, Normal copula, Gumbel copula and Frank copula. To visualize the fitted and observed values, the log-returns of the pair AMZN & BRK.B are plotted below.

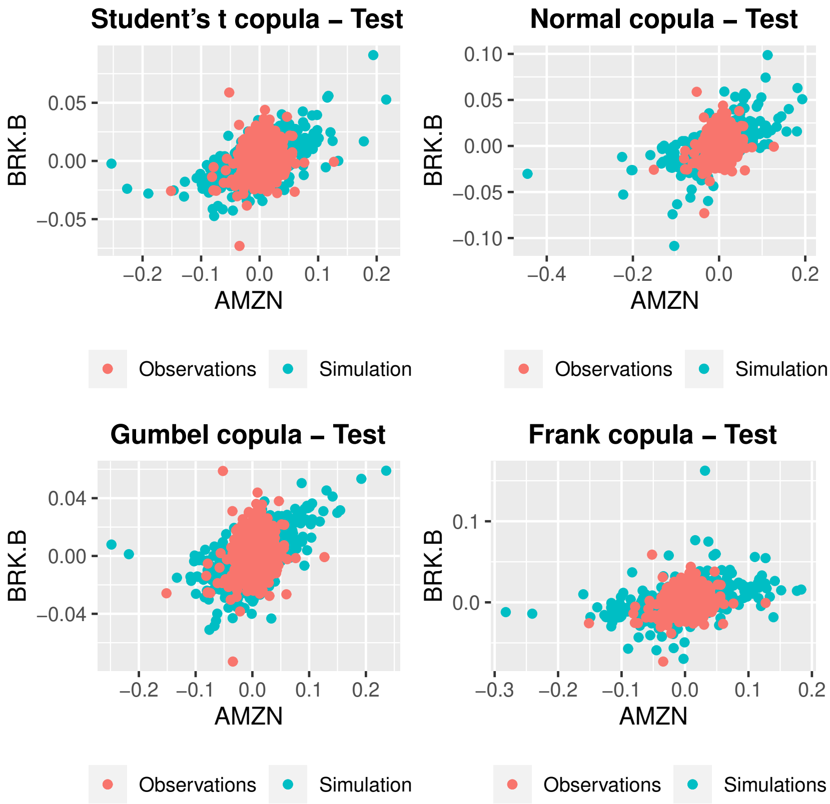

Figure 5.5: Observed vs. simulated log-returns for AMZN and BRK.B in the period from 1st of April 2020 until 31st of May 2022

It can be seen that the proposed copulas fit the data relatively well, however, they still assume heavier tails than the data possess. Moreover, it can be argued which copula performs best from a visual point of view, as all of the copulas seem to fit nicely except for the heavy tails.

Value-at-Risk Forecast

Next, one-day-ahead out-of-sample VaR is forecasted using the procedure described in Section 3.3. Again, $N = 10,000$ is chosen and $M = 194$ one-day-ahead out-of-sample forecasts are used. Afterwards, the obtained VaR forecasts are evaluated using the backtesting methods from Section 3.4. The forecasting performance of the procedure can be seen below based on the four best-fitting copulas found in Table 5.8.

	95% VaR			99% VaR		
Copula	Z/T	LR_{UC}	LR_{CC}	Z/T	LR_{UC}	LR_{CC}
Normal	0.02062	4.48785	4.65717	0.00515	0.55922	0.56963
p-val		0.03414	0.09743		0.45458	0.75215
Student's t	0.02062	4.48785	4.65717	0	3.89953	3.89953
p-val		0.03414	0.09743		0.04830	0.14231
Gumbel	0.02577	2.89197	3.15796	0.00515	0.55922	0.56963
p-val		0.08902	0.20619		0.45458	0.75215
Frank	0.02577	2.89197	3.15796	0.01546	0.50141	0.59615
p-val		0.08902	0.20619		0.47888	0.74225

Table 5.9: Value-at-Risk forecast performance - Test set

The table shows that the Gumbel copula and Frank copula are closest to the desired ratio of VaR exceedances for the 95% VaR, whereas the Frank copula is closest for the 99% VaR. Moreover, it can be seen that Kupiec's unconditional coverage test rejects the null hypothesis for the Normal copula and t-copula for the 95% VaR and for the t-copula for the 99% VaR. Christoffersen's independence test fails to reject the null hypothesis for all four copulas for the 95% and 99% VaR. Again, the results do not coincide with those found in Table 5.8.

Next, the loss functions are used to determine which copula performs best. Both the loss function provided by Lopez and the loss function provided by Blianco and Ihle are used. The results of the loss functions for the 95% and 99% VaR are shown below.

	95% VaR		99% VaR	
Copula	$\hat{C}^L$	$\hat{C}^{BI}$	$\hat{C}^L$	$\hat{C}^{BI}$
Normal	0.14934	0.00582	0.00553	0.00012
Student's t	0.15355	0.00602		
Gumbel	0.25662	0.00986	0.03628	0.00138
Frank	0.24243	0.00927	0.07433	0.00233

Table 5.10: Loss functions - Test set

It can be seen from the table that the lowest value of $\hat{C}^L$ and $\hat{C}^{BI}$ are found for the Normal copula for both the 95% and the 99% VaR. Note that the loss functions are not calculated for the t-copula in the 99% VaR, as Z/T was found to be zero in this case.

To illustrate the predictive performance of the VaR, the portfolio returns as well as the 95% VaR, and 99% VaR, are plotted in Figure 5.6. The figure shows the forecasts based on the Monte Carlo procedure for the Normal copula, Gumbel copula and Frank copula.

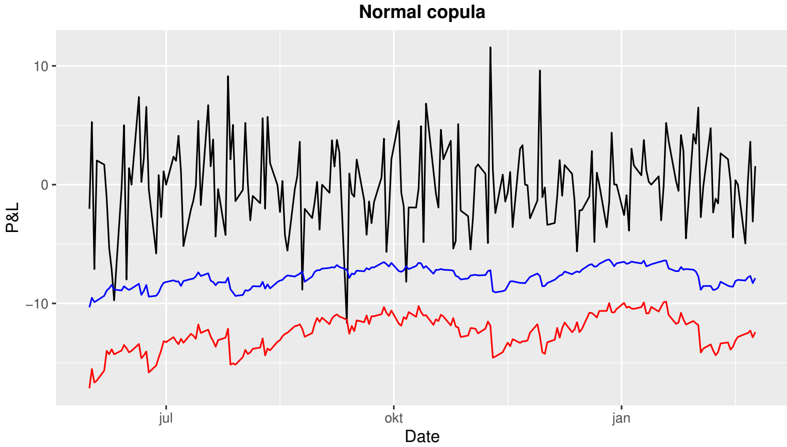

(a) Forecast performance with the Normal copula

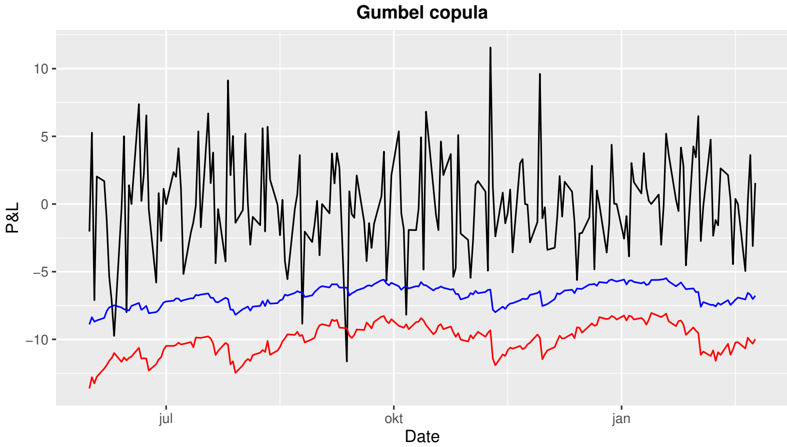

(b) Forecast performance with the Gumbel copula

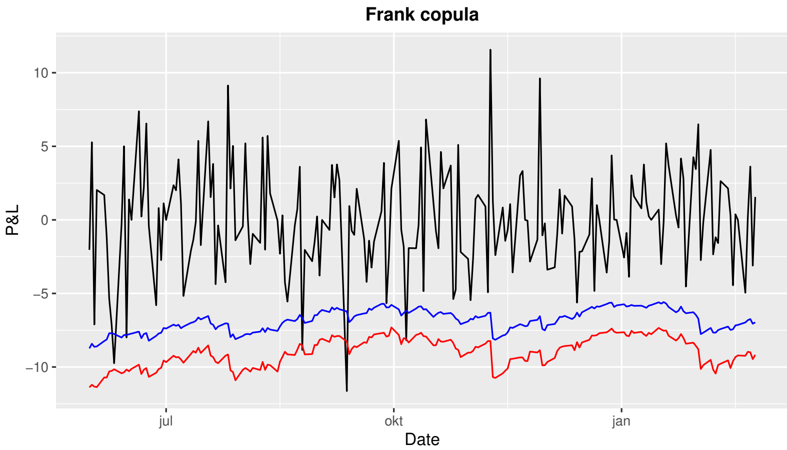

(c) Forecast performance with the Frank copula

Figure 5.6: Visualization of the P&L function with the obtained VaR forecasts from the Monte Carlo procedure. The blue curve represents the 95% VaR and the red curve represents the 99% VaR.

5.2 Comparison with the S&P500 Index

This section is inspired by [Wang et al., 2022], [Kelepouris and Kelepouris, 2019] and [Ruppert and Matteson, 2015, page 558].

In this section, an analysis of the Value-at-Risk of the S&P500 index will be conducted. This is done to compare the results with those obtained from the analysis of the self-constructed equally weighted portfolio consisting of the 10 biggest assets of the S&P500 index in Chapter 4. In this section, the VaR forecasts will be constructed based on the parametric VaR estimation described in Section 3.2. First, the data will be described, next the ARMA-GARCH models will be fitted to the index and lastly the VaR will be forecasted and evaluated.

The chosen data is collected from [Nasdaq, 2023] and consists of the daily closing prices of the S&P500 index in the period from the 1st of May 2013 until the 27th of February 2023, thus consisting of $2,512$ observations. Note that this period is shorter than the period used for the portfolio, as it was only possible to obtain the daily closing prices of the index for this shorter period. The data is split into a train and test set, with the train set consisting of daily data in the period from the 1st of May 2013 until the 31st of March 2020 with a total of $1,765$ observations. The test set consists of daily data in the period from the 1st of April 2020 until the 27th of February 2023, thus a total of 759 observations. Note that the test set of the index is the same size as the test set of the portfolio. This is done to ensure consistency in regard to the forecasted VaR. A plot of the daily closing prices of the S&P500 index can be seen below with the dotted line indicating the division between the train and test set.

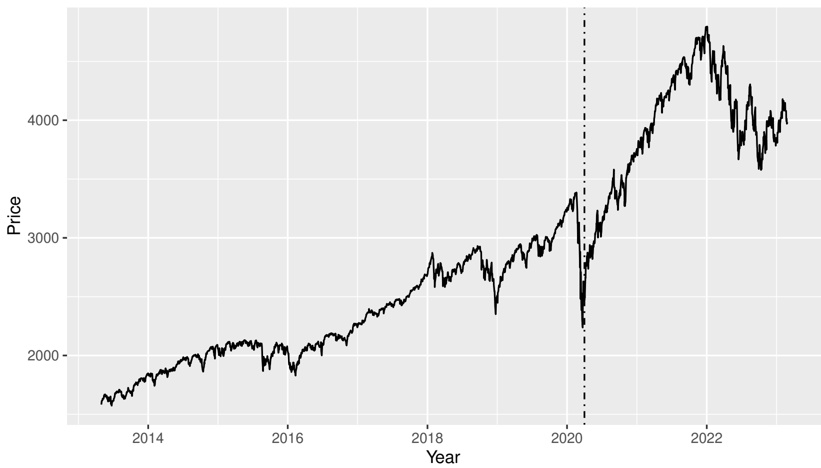

Figure 5.7: Index prices from 1st of May 2013 until 27th of February 2023. The dotted line represents the division between the train and test set.

It can be seen that the prices of the index resemble the prices of the portfolio seen in Figure 4.1. However, for obvious reasons, the scale of the prices is higher for the index than for the portfolio. Moreover, it can be seen that the index prices contain more volatility than the portfolio prices at the very beginning of the period. It can still be seen that the prices are slowly increasing throughout the train set, whereafter they decline drastically just around the beginning of 2020. Once again, it can be seen that the test set contains more volatility than the train part. However, it can be argued that the behaviour of the train and test set is more alike for the index prices than for the portfolio prices as volatility is seen throughout the full period. This will possibly result in better results in regard to VaR forecasting.

To be able to fit ARMA-GARCH models on the index, the daily prices are converted to log-returns, to ensure stationarity. The log-returns of the index are shown below for the full sample:

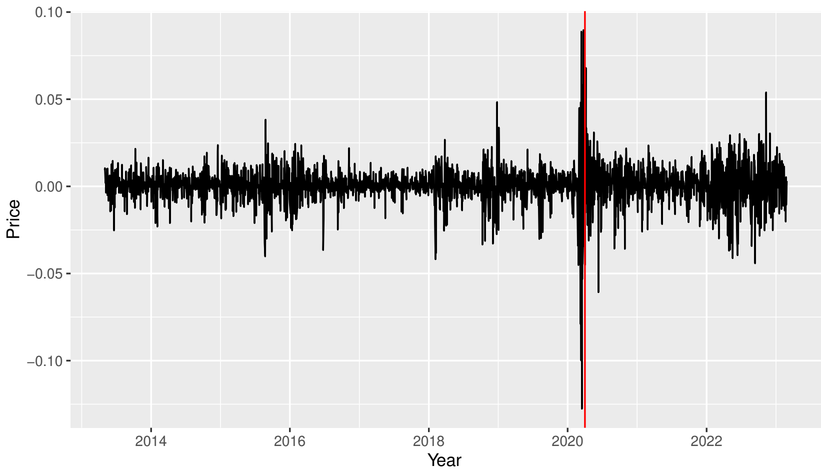

Figure 5.8: Index log-returns from 1st of May 2013 until 27th of February 2023. The red line indicates the division between the train and test set.

It can be seen that the log-returns of the index seem pretty stationary around 0, however with large fluctuations around the beginning of 2020. Moreover, it can be seen that the most volatility clustering is present around 2016 as well as in 2022 and 2023, and the volatility clusterings seem to represent those found for the 10 assets of the portfolio in Figure 4.2.

To investigate the log-returns further, the descriptive statistics have been computed for both the full sample, train set and test set. The statistics can be seen in the below table.

	Full Sample	**Train Set**	**Test Set**
Mean	0.00037	0.00028	0.00057
St. Deviation	0.01111	0.01044	0.01253
95% VaR	-0.0168	-0.0147	-0.0206
99% VaR	-0.0330	-0.0310	-0.0358
Skewness	-0.83132	-1.28224	-0.21695
Excess Kurtosis	16.68897	28.04336	2.63401
Jarque-Bera	$29,570$	$58,286$	225.37
P-value	$< 2.2e^{-16}$	$< 2.2e^{-16}$	$< 2.2e^{-16}$
ADF test	-13.820	-12.191	-9.570
P-value	0.01	0.01	0.01
Ljung-Box	50.683	66.596	3.073
P-value	$1.09e^{-12}$	$< 3.33e^{-16}$	0.0796

Table 5.11: Descriptive statistics of the log-returns - Index

It can be seen from the table that the means are approximately 0 for all three samples, however, they are smaller in the train set than in the test set. Moreover, the standard deviations are approximately the same in all three periods. The historical 95% and 99% VaR values are negative for all three periods and approximately on the same level as for the portfolio.

In regards to skewness, it can be seen that the index is left-skewed, and the most skewness is seen in the train set. The test for excess kurtosis supports this result. Moreover, the Jarque-Bera test rejects the null hypothesis of normally distributed data in all three samples. The ADF test supports the stationarity seen in Figure 5.8, as it rejects the null hypothesis in all three periods. Lastly, the Ljung-Box test rejects the null hypothesis in all three samples indicating that the assets contain autocorrelation. To investigate the distribution of the index further, a Q-Q plot is given below for the full sample.

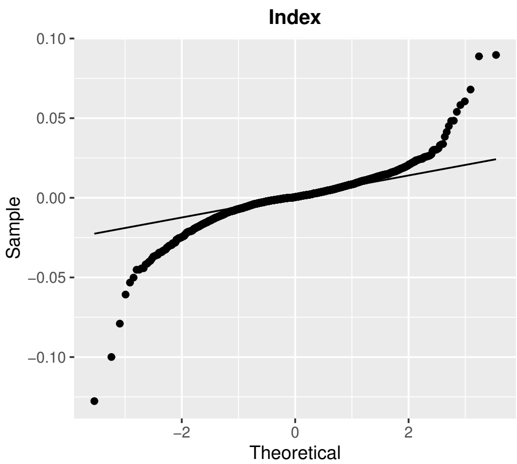

Figure 5.9: Q-Q plot of the index based on the full sample

It can be seen from Figure 5.9 that the index does posses heavy tails. However, the tails are smaller than those of AMZN, META, NVDA, TSLA, UNH and AAPL from the portfolio, as seen in Figure 4.3. As stated earlier, the ARMA-GARCH models are a reasonable choice for modelling the tails. Thus, these are fitted on the training set. Again, an ARMA$(0,0)$-GARCH$(1,1)$ model and an ARMA$(1,1)$-GARCH$(1,1)$ model is fitted assuming that the standardized residuals are either normally distributed, t-distributed, or skewed t-distributed. The log-likelihood, AIC, and BIC values can be seen in the below table.

	ARMA(0,0)-GARCH(1,1)			**ARMA(1,1)-GARCH(1,1)**		
	Normal	t	Skewed t	Normal	t	Skewed t
LL	$8,168.20$	$8,267.95$	$8,257.35$	$8,172.35$	$8,262.95$	$8,257.29$
AIC	-6.739	-6.812	-6.809	-6.741	-6.812	-6.812
BIC	-6.729	-6.800	-6.800	-6.726	-6.800	-6.800

Table 5.12: Model selection criteria - Index

It can be seen that the ARMA$(0,0)$-GARCH$(1,1)$ model with t-distributed standardized residuals results in the highest log-likelihood and lowest AIC and BIC values of the six tested models. To test whether it is reasonable to fit an ARMA-GARCH model, and not just an ARMA model, the heteroskedasticity of the ARMA$(0,0)$ model is checked. The results can be seen in the table below.

Ljung-Box test on the squared residuals		
ARMA$(0,0)$		
	Q-stat.	P-value
Lag 5	$3,138.9$	$< 2.2e^{-16}$
Lag 10	$4,335.6$	$< 2.2e^{-16}$
Lag 15	$5,375.6$	$< 2.2e^{-16}$

Table 5.13: Test for heteroskedasticity in the residuals of the ARMA$(0,0)$ model - Index

It can be seen that the Ljung-Box test rejects the null hypothesis of no autocorrelation for both lag 5, 10 and 15. Thus, it is reasonable to assume that ARMA-GARCH models are more representative of the data than just ARMA models. The parameter estimates and statistical tests for the ARMA-GARCH model can be seen below.

Parameter estimates and statistic tests		
	Value	P-value
μ	0.0009	0.000
ω	0.0000	0.056
α	0.2139	0.000
β	0.7848	0.000
ν	5.0548	0.000
Ljung-Box test on the standardized residuals		
	Q-stat.	P-value
Lag 5	2.3705	0.7959
Lag 10	5.9715	0.8177
Lag 15	10.566	0.7827
Ljung-Box test on the squared standardized residuals		
	Q-stat.	P-value
Lag 5	5.1628	0.3963
Lag 10	11.000	0.2897
Lag 15	14.600	0.4806

Table 5.14: Estimation results for the index

It can be seen that all parameters except ω are significant for the model. In regards to the statistical tests, the Ljung-Box test fails to reject the null hypothesis for both the standardized residuals and the squared standardized residuals for all three lags. This indicates that the distribution seems to be nicely fitted.

Next, Value-at-Risk forecasting will be performed. The process is as follows:

1. Use the estimation sample with T observations to fit the respective ARMA-GARCH models on the log-returns.

2. Forecast one-step ahead means, $\hat{r}_{T+1}$, and variances, $\hat{\sigma}_{T+1}$, at time $T+1$.

3. Use the degree of freedom found in Step 1. to find the critical value z for the 95% VaR and the 99% VaR.

4. Use the values from steps 1.-3. to compute the forecasted Value-at-Risk by use of (3.1). In the case of t-distributed innovations, the formula of the parametric VaR is given as

$$VaR^{par,t}(\alpha) = r_t \times (\hat{r}_{T+1} + \hat{q}_{\alpha,t}(\hat{\nu})\hat{\sigma}_{T+1}),$$

   where r_t represents the log-returns at time t and $\hat{q}_{\alpha,t}(\hat{\nu})$ is the α-quantile of the t-distribution with tail index $\hat{\nu}$.

5. Convert VaR from log-returns to returns by

$$R_t = P_{t-1}(\exp(r_t) - 1),$$

where R_t indicates the returns, P_t the prices and r_t the log-returns, all at time t.

6. Repeat steps 1.-5. M times by rolling over the daily returns, where M is the number of days needed to be forecasted.

After the 95% VaR and 99% VaR have been computed for $M = 759$ the backtesting is performed. However, the loss functions are not computed, as they act as a goodness-of-fit measure and thus are not relevant to compute when having only one model. The results of the ratio of VaR exceedances, Z/T, Kupiec's unconditional coverage test, LR_{UC}, and Christoffersen's independence test, LR_{CC}, are given below for the 95% VaR and 99% VaR.

	95% VaR			99% VaR		
	Z/T	LR_{UC}	LR_{CC}	Z/T	LR_{UC}	LR_{CC}
Index	0.07510	8.78091	8.80370	0.01449	1.35890	1.68287
P-value		0.00304	0.01225		0.24373	0.43109

Table 5.15: Value-at-Risk forecast performance - Index

The table shows that the ratio of VaR exceedances is higher than the expected ratio of exceedances for both the 95% VaR and the 99% VaR. This is in contrast to the results found for the portfolio, where they were lower than the expected ratio of exceedances. In regards to Kupiec's unconditional coverage test and Christoffersen's independence tests, they reject the null hypothesis for the 95% VaR, whereas they fail to reject it for the 99% VaR. This is in contrast to the results found for the portfolio, for which the tests rejected the null hypothesis for all four copulas in the 95% VaR, and for all copulas except the Frank copula in the 99% VaR. Thus, the performance of the index is better than that of the portfolio in regard to the likelihood tests.

To illustrate the predictive performance of the index's VaR, the index returns, as well as the 95% VaR and 99% VaR, are plotted below in Figure 5.10.

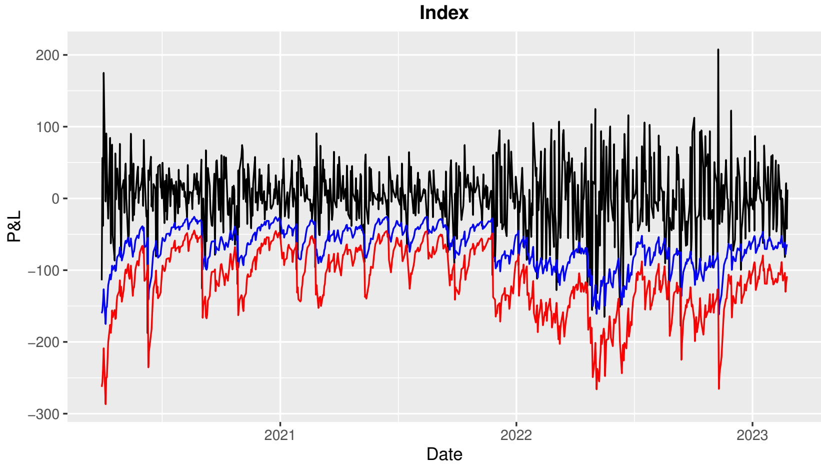

Figure 5.10: Visualization of the index's P&L function with the calculated VaR forecasts. The blue curve represents the 95% VaR and the red curve represents the 99% VaR.

Discussion 6

When modelling the marginal distributions in the project, two different marginal models have been proposed; The ARMA$(0, 0)$-GARCH$(1, 1)$ and the ARMA$(1, 1)$-GARCH$(1, 1)$. These were chosen, since they are popular choices in regards to analyzing time series data, as they are the simplest and most robust among volatility models, fits many data series well, and are sufficient to capture the volatility clustering in the data [Ghani and Rahim, 2018]. However, it can be argued whether other models should have been tested as well. This could for example be by including more lags in the models and thus testing other combinations of the ARMA-GARCH models. Moreover, other types of volatility models could be proposed e.g. the GJR-GARCH model, also known as the Threshold GARCH. This model is proposed to capture an asymmetric behaviour by allowing the current conditional variance to have a different response to the past positive and negative returns [Nugroho et al., 2019].

In regards to the fitting of the marginal distributions for the train and test set, it was found from Table A.2 and Table A.6 that the Ljung-Box test fails to reject the null hypothesis for GOOGL in the train set and META in the test set. Thus, in these cases, GARCH effect was not found to be present. However, for the sake of the project, it was chosen to model these assets by an ARMA-GARCH model either way. It can be discussed whether this was the best decision, as this might have influenced the obtained model fit and thereby the estimated Value-at-Risk values.

When evaluating the model fit of the marginal distributions, the decision was made based on the BIC value instead of the log-likelihood and AIC value. Most times they all agreed on the model fit, however sometimes the AIC and likelihood disagreed with the BIC. In these cases, the BIC was chosen as it penalizes the complexity of the models more than the AIC does [Lin, 2021]. The choice of model criteria has influenced which marginal models were fitted. Thus, it might also have influenced the estimated copula and therefore the obtained Value-at-Risk estimates.

In the Monte-Carlo Value-at-Risk forecasting procedure, it was chosen to simulate the standardized residuals $N = 10,000$ times for each out-of-sample forecast. This was chosen as it is important to let N be large, but not too large for computational reasons. However, the size of N is a popular topic of discussion, as mentioned in [Lu et al., 2011]. It is reasonable to assume that the fit of the copulas would be better in regards to the chosen data if the size of N was chosen to be higher, e.g. $N = 100,000$. However, for computational reasons, this was not possible to attain within the time frame of the project.

In Section 5.2 the Value-at-Risk is forecasted for the S&P500 index in order to compare the results with those obtained from the portfolio in Chapter 4. However, it can be argued whether this comparison is reasonable since the two forecasting methods differ. It is reasonable to believe that the obtained results would have been more similar if the Value-at-Risk had been based on the parametric estimation method for both the portfolio and the index. However, since the point of the project has been to fit copula-GARCH models on the portfolio, the parametric estimation of the Value-at-Risk has not been performed for the portfolio.

Finally, it can be discussed whether the chosen data is the best possible data set to evaluate the Value-at-Risk. It can be seen from Figure 4.1 that the prices behave very differently throughout the period. In particular, the periods of the train and test sets can be discussed, as they behave very differently. It can be argued that the choice of periods may have influenced the model fits and thus the forecasted Value-at-Risk estimations. Moreover, the length of the data set can be argued, as it is difficult to obtain great model fits on too long periods of data, as the possibility of different behaviour throughout the period is larger. This is supported by the fact that the obtained VaR models in the test period, which is the shortest tested period, behaved drastically better than in the full data set and train set. However, in order to evaluate the forecasted Value-at-Risk values, the length of the data set should not be too short either.

Conclusion 7

In this project, it has been examined how to estimate the Value-at-Risk of an equally weighted portfolio consisting of the 10 largest assets of the S&P500 index. In order to do so, theory regarding copula models has been presented. The theory included definitions and theorems of copula models, with the main theorem being Sklar's Theorem presented in Theorem 2.1. This theorem states that any multivariate joint distribution can be written in terms of univariate marginal distribution functions and a copula that describes the dependence structure between the variables. This theorem was used to construct the equally weighted portfolio. Moreover, multiple examples of different copulas have been presented, which were all used to construct the best-fitting models in Chapter 4 and 5. Additionally, tail dependency and calibration of copulas were described.

Since the daily closing prices of the 10 assets of the equally weighted portfolio were seen to be very volatile in Figure 4.1, the choice was made to model the marginal distributions as ARMA-GARCH models. This was chosen as the GARCH model is a popular way of modeling volatility clustering and heavy tails in time series.

The risk estimation has been based on the Value-at-Risk measure, which is one of the most popular and widely used approaches to risk estimation. Three different estimation methods were presented; Historical estimation, parametric estimation and Monte-Carlo estimation. Both the historical estimation method and the Monte-Carlo estimation method were used to evaluate the risk of the equally weighted portfolio. The parametric estimation method was used to evaluate the risk of the S&P500 index in order to compare the risk of the portfolio to the risk of the index. Moreover, multiple backtesting techniques were presented, which were used to evaluate the performance of the forecasted Value-at-Risk estimates obtained by the Monte-Carlo estimation method.

The 95% and 99% Value-at-Risk of the equally weighted portfolio was estimated on three different periods; the full period containing daily closing prices in the period from the 1st of June 2012 until the 27th of February 2023, the training period consisting of daily closing prices in the period from the 1st of June 2012 until the 31st of March 2020 and lastly the test period containing daily closing prices from the 1st of April 2020 until the 27th of February 2023. Both the performance of the observed ratio of VaR exceedances, Z/T, Lopez's loss function, $\hat{C}^L$, and Bianco and Ihle's loss function, $\hat{C}^{BI}$, were evaluated. Moreover, Kupiec's unconditional coverage test and Christoffersen's independence test were performed. The evaluation based on the different proposed copula-GARCH models resulted in the following conclusions for each of the three periods:

- Full period: The Normal copula resulted in the lowest $\hat{C}^L$ and $\hat{C}^{BI}$ values for the 95% VaR, whereas the Gumbel and Frank copulas provided the best results of Z/T for the 95% VaR and 99% VaR, respectively. Both Kupiec's unconditional test and Christoffersen's independence test rejected the null hypothesis for all copulas except for the Frank copula for the 99% VaR.
- Train period: The t-copula resulted in the lowest value of $\hat{C}^L$ and $\hat{C}^{BI}$ for both the 95% VaR and 99% VaR. In regards to the expected ratio of VaR exceedances, the Frank copula performed best for both the 95% VaR and 99% VaR. Kupiec's unconditional test rejected the null hypothesis for the Normal copula and t-copula for the 95% VaR and 99% VaR, whereas Christoffersen's independence test only rejected the null hypothesis for the Normal copula and t-copula for the 95% VaR.
- Test period: The Normal copula resulted in the lowest $\hat{C}^L$ and $\hat{C}^{BI}$ for both the 95% VaR and 99% VaR. The Gumbel copula and Frank copula both resulted in the best Z/T value for the 95% VaR, whereas the Frank copula resulted in the best Z/T value for the 99% VaR. Kupiec's unconditional coverage test rejected the null hypothesis for the Normal copula and t-copula for the 95% VaR and for the t-copula for the 99% VaR. Christoffersen's independence test did not reject the null hypothesis in any situation.

For all three time periods, the observed VaR exceedances were found to be lower than the expected ratio of exceedances for both the 95% VaR and 99% VaR. Thus, the risk of the portfolio is overestimated.

In regards to the parametric Value-at-Risk estimation of the S&P500 index, it was found that the observed ratio of VaR exceedances was higher than the expected ratio of exceedances for both the 95% VaR and 99% VaR. This means that the risk of the index is underestimated. Moreover, Kupiec's unconditional coverage test and Christoffersen's independence test rejected the null hypothesis for the 95% VaR, whereas they failed to reject the null hypothesis for the 99% VaR. Thus, both tests accept the null hypothesis more often for the index than for the portfolio.

8 Reflection

The main focus of the project has been Value-at-Risk estimation based on constructed copula-GARCH models. However, it could be of interest to investigate whether other marginal distributions would provide a better fit for the data. A popular choice of distribution is the Normal Inverse Gaussian (NIG) distribution, which is defined in Appendix A.2. This distribution is found to fit daily stuck returns nicely, as it incorporates fat tails and skewness by including a spread parameter [Kucharska and Pielaszkiewicz, 2009]. It could be interesting to see whether this distribution would fit the daily log-returns of the assets nicely, as it was found in Table 4.2 and Figure 4.3 that all 10 assets contain skewness and heavy tails in the full sample.

Another approach could have been to investigate other copula functions. It was seen in Figure 4.4 that neither of the proposed copulas was found to fit the data particularly nicely. It could be a possibility that other copula models, e.g. time-varying copula models, could have resulted in a better fit. This is for example seen in [Lu et al., 2011], where the time-varying copulas perform better than the stationary copula models in regards to the goodness-of-fit. Thus, this could also be thought to be the case with the portfolio which is analyzed in this project. If a better fit was found in regard to the copula modelling, it is possible that a better VaR forecasting performance would have been obtained. However, given the time frame of the project, it was not possible to investigate and compare more copulas than those proposed in Section 2.1.

In regards to the Value-at-Risk calculations, only a time horizon of one day has been considered. However, it could have been interesting to analyze other periods than just one day ahead, e.g. one week, one month, or even one year ahead. As the data is very volatile and both increases and decreases significantly throughout the period, it is reasonable to assume that the choice of time horizon would influence the forecasted Value-at-Risk values and performance of the tested models.

In regards to the analyzed portfolio, it could also be of interest to observe other portfolios to compare the model fits and Value-at-Risk forecasts. An approach is that the portfolio could have been built such that it was not equally weighted but instead more representative of the proportion of the S&P500 index. This could have been done by letting the weight of the individual assets of the portfolio be given as the ratio of the index as given by Table 4.1. Hence, AAPL should have taken up the most weight and UNH the least weight. This would most likely result in other estimated VaR values since the weight of the individual assets is far from equally weighted in the S&P500 index. Moreover, it could also lead to different results in regard to the copula modelling. These forecast results could also be imagined to be more alike to those found from analyzing the index in Section 5.2.

Another approach in regard to the construction of the portfolio is to look at assets from the different GICS sectors. It can be seen from Table 4.1 that six of the 10 assets are in the sectors "Information Technology" and "Communication Services", which are closely related. Thus, the similarity of the assets can be thought to have affected the fitted models. A portfolio including assets from all 11 sectors would reflect the diversity of the S&P500 index better than the constructed portfolio. Moreover, the Value-at-Risk forecasts are imagined to provide better results for a diversified portfolio than for a portfolio that is not diversified.

In regards to the risk estimation, other risk measures could have been observed. A possibility is to evaluate the risk based on the conditional Value-at-Risk (CVaR) instead of the Value-at-Risk. The CVaR is a risk measure that quantifies the amount of tail risk in an investment portfolio and it is derived by taking a weighted average of the extreme losses in the tail of the distribution of possible returns beyond the VaR cutoff point. Thus,

$$CVaR(\alpha) = \frac{\int_0^\alpha VaR(u)du}{\alpha},$$

which is the average of $VaR(u)$ over all u that are less than or equal to α [Ruppert and Matteson, 2015, pp. 554]. The advantage of CVaR compared to VaR is the fact that it is a coherent risk measure, as defined in Appendix A.3, which VaR is not. The CVaR is defined to be the mean loss of portfolio value given that a loss is occurring at or below the given q-quantile. The use of CVaR could be imagined to result in different estimated risk values and performance of the models.

Appendix A

A.1 Jarque-Bera Test

This section is based on [Ruppert and Matteson, 2015, pp. 91-92].

The Jarque-Bera test is used to test for the normality of the data. This is done by comparing the sample skewness and kurtosis to 0 and 3, which are the respective values under normality. The test statistic is given as

$$JB = n\left[\frac{\widehat{Sk}^2}{6} + \frac{(\widehat{Kur}-3)^2}{24}\right],$$

where $\widehat{Sk}$ is the sample skewness and $\widehat{Kur}$ is the sample kurtosis. The test statistic is 0 when $\widehat{Sk}$ and $\widehat{Kur}$ are 0 and 3 respectively and increases in value as $\widehat{Sk}$ and $\widehat{Kur}$ deviate from these values.

The test statistic, JB, is distributed as $\chi^2(2)$ under the null hypothesis of normality.

A.2 Normal Inverse Gaussian Distribution

This section is based on [Pedersen, 2009, pp. 37-38].

Consider a Brownian motion with drift β, which is subordinated by the Lévy process $(S_t)_{t\geq 0}$, where $S_t \sim IG(\delta t, \rho)$; $(W_{S_t} + \beta S_t)_{t\geq 0}$. The process $(S_t)_{t\geq 0}$ is called an IG Lévy process. Now add a drift to the new Lévy process $(W_{S_t} + \beta S_t)_{t\geq 0}$, and denote it by

$$Xt = W_{S_t} + \beta S_t + \mu t, \quad t \geq 0. \tag{A.1}$$

The distribution of (A.1) can be shown to be a normal inverse Gaussian (NIG) distribution.

Definition A.1.
Let Z_t be a random variable. Then Z is said to follow a normal inverse Gaussian distribution if it has the density function

$$f(x;\alpha,\beta,\mu,\delta) = \frac{\alpha\delta}{\pi}\exp\left(\delta\sqrt{\alpha^2-\beta^2}+\beta(x-\mu)\right)\frac{K_1(\alpha\sqrt{\delta^2+(x-\mu^2)})}{\sqrt{\delta^2+(x-\mu^2)}},$$

where $\alpha,\delta > 0$, $\beta \in (-\alpha,\alpha)$, $\mu \in \mathbb{R}$ and K_1 is the modified Bessel function of third order and with index 1. The notation $Z \sim NIG(\alpha,\beta,\mu,\delta)$ is used for such a random variable.

A.3 Coherent Risk Measure

This section is based on [Elliott and Kopp, 2005, pp. 303-315].

Definition A.2 (Coherent Risk Measure).
A coherent risk measure is a function $\rho : L^1 \to \mathbb{R}$ such that

1. If $X \geq 0$, then $\rho(X) \leq 0$,
2. If $k \in \mathbb{R}$, then $\rho(X+k) = \rho(X) - k$,
3. If $\lambda \geq 0$ in $\mathbb{R}$, then $\rho(\lambda X) = \lambda\rho(X)$,
4. $\rho(X+Y) \leq \rho(X) + \rho(Y)$.

When the third property is fulfilled, the fourth property is equivalent to convexity in the following sense; Let X, Y and $0 \leq \lambda \leq 1$ be given and assume that ρ fulfils both the third and fourth property such that

$$\rho(\lambda X + (1-\lambda)Y) \leq \rho(\lambda X) + \rho((1-\lambda)Y) = \lambda\rho(X) + (1-\lambda)\rho(Y),$$

thus ρ is convex.

A.4 Plots and Figures - Train Set

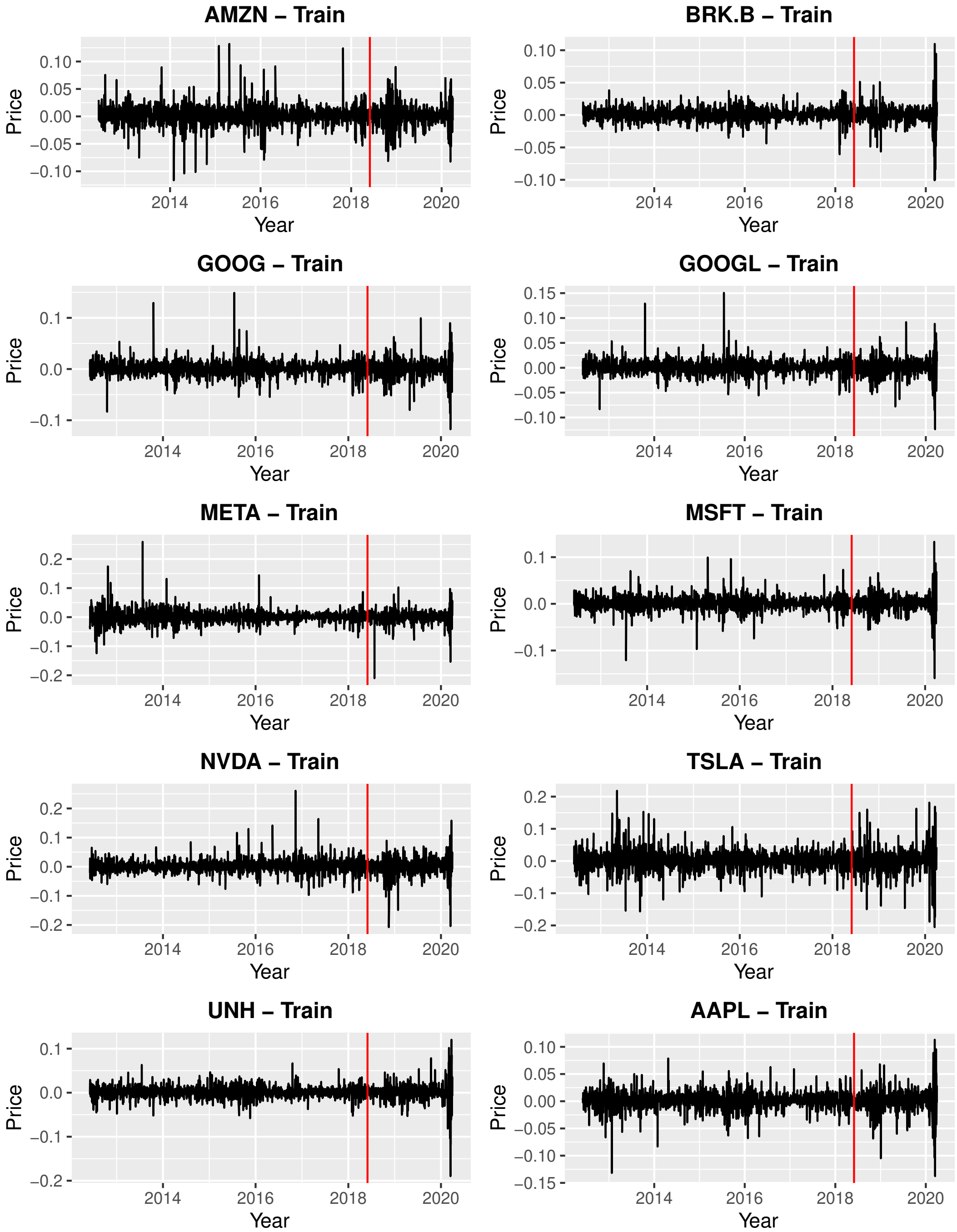

Figure A.1: Log-returns from 2st of June 2012 until 31st of March 2020. The red lines indicate the division between the train and test set.

Train Set	**AMZN**	**BRK.B**	**GOOG**	**GOOGL**	**META**	**MSFT**	**NVDA**	**TSLA**	**UNH**	**AAPL**
Mean	0.00132	0.00057	0.00088	0.00088	0.00124	0.00081	0.00196	0.00149	0.00095	0.00055
St. Deviation	0.0178	0.0094	0.0138	0.0137	0.0219	0.0140	0.0214	0.0290	0.0127	0.0152
95% VaR	−0.0241	−0.0136	−0.0203	−0.0209	−0.0312	−0.0193	−0.0290	−0.0432	−0.0183	−0.0242
99% VaR	−0.0436	−0.0237	−0.0368	−0.0366	−0.0557	−0.0378	−0.0553	−0.0759	−0.0356	−0.0423
Skewness	0.3362	−0.1531	1.1160	1.0752	1.4833	−0.1476	1.6600	0.3376	−0.0209	−0.5190
Excess Kurtosis	13.033	6.097	18.625	18.893	21.524	12.959	22.060	8.842	5.572	9.511
Jarque-Bera	6594	631	16,244	16,772	22,949	6473	24,407	2255	431	2835
P-value	$< 2.2e^{-16}$	$< 2.2e^{-16}$	$< 2.2e^{-16}$	$< 2.2e^{-16}$	$< 2.2e^{-16}$	$< 2.2e^{-16}$	$< 2.2e^{-16}$	$< 2.2e^{-16}$	$< 2.2e^{-16}$	$< 2.2e^{-16}$
ADF test	−11.778	−11.912	−13.040	−12.919	−11.718	−13.029	−13.220	−11.140	−13.368	−12.577
P-value	0.01	0.01	0.01	0.01	0.01	0.01	0.01	0.01	0.01	0.01
Ljung-Box	18.871	31.413	27.188	25.355	8.333	29.207	28.226	11.116	18.772	22.983
P-value	0.170	0.004	0.018	0.031	0.871	0.010	0.013	0.677	0.174	0.061
Test Set	**AMZN**	**BRK.B**	**GOOG**	**GOOGL**	**META**	**MSFT**	**NVDA**	**TSLA**	**UNH**	**AAPL**
Mean	$3.61e^{-4}$	$-1.05e^{-4}$	$7.96e^{-5}$	$4.92e^{-5}$	$-3.17e^{-4}$	$9.39e^{-4}$	$4.81e^{-5}$	$1.23e^{-3}$	$5.13e^{-5}$	$6.08e^{-4}$
St. Deviation	0.0202	0.0163	0.0192	0.0191	0.0240	0.0207	0.0333	0.0419	0.0226	0.0221
95% VaR	−0.0326	−0.0194	−0.0282	−0.0271	−0.04313	−0.0316	−0.0484	−0.0547	−0.0306	−0.0326
99% VaR	−0.0606	−0.0513	−0.0572	−0.0576	−0.0683	−0.0552	−0.1090	−0.1460	−0.0593	−0.0678
Skewness	−0.1065	−0.3640	−0.4563	−0.5845	−1.8889	−0.5015	−1.1333	−0.1671	−0.9613	−0.6239
Excess Kurtosis	6.3215	17.5798	10.2673	10.3532	20.1937	16.1133	11.2175	8.7550	18.8127	10.9140
Jarque-Bera	220.2	4235.4	1066.2	1101.8	6159.2	3437.6	1444.2	660.5	5043.1	1275.8
P-value	$< 2.2e^{-16}$	$< 2.2e^{-16}$	$< 2.2e^{-16}$	$< 2.2e^{-16}$	$< 2.2e^{-16}$	$< 2.2e^{-16}$	$< 2.2e^{-16}$	$< 2.2e^{-16}$	$< 2.2e^{-16}$	$< 2.2e^{-16}$
ADF test	−9.0120	−7.4994	−8.1680	−8.1002	−8.2291	−8.5605	−8.5873	−7.3412	−10.8220	−7.6448
P-value	0.01	0.01	0.01	0.01	0.01	0.01	0.01	0.01	0.01	0.01
Ljung-Box	34.09	187.38	104.11	109.37	42.26	181.43	47.61	11.29	168.16	105.13
P-value	0.0020	$< 2.2e^{-16}$	$7.77e^{-16}$	$< 2.2e^{-16}$	0.0001	$< 2.2e^{-16}$	$1.53e^{-55}$	0.6629	$< 2.2e^{-16}$	$4.44e^{-16}$

Table A.1: Descriptive statistics of the log-returns - Original train set

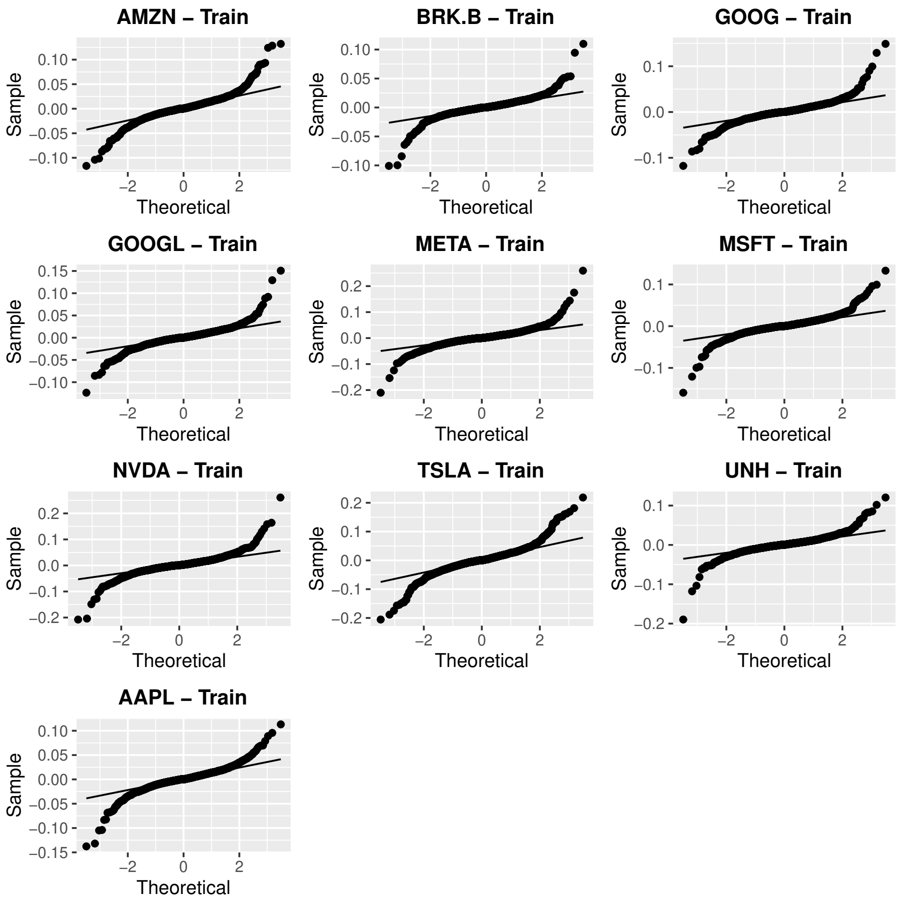

Figure A.2: Q-Q plots based on the original train set

Ljung-Box test on the squared residuals of the ARMA models - Original train set										
	AMZN		**BRK.B**		**GOOG**		**GOOGL**		**META**	
Lag	ARMA(0,0)		ARMA(0,0)		ARMA(0,0)		ARMA(0,0)		ARMA(0,0)	
	Q-stat.	P-value	Q-stat.	P-value	Q-stat.	P-value	Q-stat.	P-value	Q-stat.	P-value
5	12.1	0.0335	508.9	$< 2e^{-16}$	11.9	0.0367	7.6	0.1821	15.7	0.0078
10	22.7	0.0119	536.9	$< 2e^{-16}$	17.0	0.0747	12.414	0.2583	19.12	0.0388
15	25.2	0.0470	553.6	$< 2e^{-16}$	18.0	0.2643	13.5	0.5642	26.1	0.0374
	MSFT		**NVDA**		**TSLA**		**UNH**		**AAPL**	
Lag	ARMA(0,0)		ARMA(0,0)		ARMA(0,0)		ARMA(0,0)		ARMA(0,0)	
	Q-stat.	P-value	Q-stat.	P-value	Q-stat.	P-value	Q-stat.	P-value	Q-stat.	P-value
5	17.5	0.0037	14.3	0.0136	115	$< 2e^{-16}$	50.3	$1.23e^{-9}$	13.4	0.0196
10	20.8	0.0223	14.6	0.1458	125.3	$< 2e^{-16}$	57.3	$1.17e^{-8}$	27.506	0.0022
15	22.8	0.0885	15.8	0.3978	163.3	$< 2e^{-16}$	67.2	$1.4e^{-8}$	51.3	$7.4e^{-6}$

Table A.2: Test for heteroskedasticity in the residuals of the ARMA models - Original train set

Parameter estimates of the marginal distributions and statistic tests - the first 5 assets										
	AMZN		**BRK.B**		**GOOG**		**GOOGL**		**META**	
	ARMA(0,0)		ARMA(0,0)		ARMA(0,0)		ARMA(0,0)		ARMA(0,0)	
	Value	P-value	Value	P-value	Value	P-value	Value	P-value	Value	P-value
μ	0.001	0.000	0.001	0.005	0.001	0.004	0.001	0.002	0.001	0.001
ω	0.000	0.011	0.000	0.000	0.000	0.249	0.000	0.250	0.000	0.574
α	0.106	0.005	0.153	0.000	0.009	0.000	0.009	0.000	0.036	0.000
β	0.724	0.000	0.679	0.000	0.985	0.000	0.986	0.000	0.961	0.000
ν	3.534	0.000	6.511	0.000	3.725	0.000	3.957	0.000	3.845	0.000
Ljung-Box test on the standardized residuals										
Lag	Q-stat.	P-value	Q-stat.	P-value	Q-stat.	P-value	Q-stat.	P-value	Q-stat.	P-value
5	6.747	0.240	10.272	0.068	3.914	0.562	4.372	0.497	3.162	0.675
10	11.756	0.302	15.359	0.120	15.053	0.130	13.961	0.175	6.410	0.780
15	17.686	0.280	17.832	0.272	16.648	0.340	15.849	0.392	9.233	0.865
Ljung-Box test on the squared standardized residuals										
Lag	Q-stat.	P-value	Q-stat.	P-value	Q-stat.	P-value	Q-stat.	P-value	Q-stat.	P-value
5	0.916	0.969	2.806	0.730	2.068	0.840	1.118	0.953	0.120	1
10	1.673	0.998	5.874	0.826	2.680	0.988	1.651	0.998	0.422	1
15	2.095	1	8.067	0.921	3.111	1	2.055	1	0.624	1

Table A.3: Estimation results for the first 5 assets of the chosen models - Original train set

Parameter estimates of the marginal distributions and statistic tests - the last 5 assets										
	MSFT		**NVDA**		**TSLA**		**UNH**		**AAPL**	
	ARMA(0,0)		ARMA(0,0)		ARMA(0,0)		ARMA(0,0)		ARMA(0,0)	
	Value	P-value	Value	P-value	Value	P-value	Value	P-value	Value	P-value
μ	0.001	0.012	0.001	0.003	0.001	0.013	0.001	0.001	0.001	0.003
ω	0.000	0.416	0.000	0.042	0.000	0.000	0.000	0.474	0.000	0.359
α	0.047	0.001	0.012	0.000	0.032	0.000	0.028	0.000	0.030	0.000
β	0.936	0.000	0.981	0.000	0.955	0.000	0.966	0.000	0.968	0.000
ν	3.426	0.000	3.425	0.000	3.640	0.000	4.501	0.000	3.597	0.000
Ljung-Box test on the standardized residuals										
Lag	Q-stat.	P-value	Q-stat.	P-value	Q-stat.	P-value	Q-stat.	P-value	Q-stat.	P-value
5	5.119	0.402	3.316	0.651	1.748	0.883	5.030	0.412	4.745	0.448
10	12.559	0.249	9.743	0.463	5.812	0.831	8.915	0.540	6.808	0.744
15	19.357	0.198	15.775	0.397	8.423	0.906	13.247	0.583	17.885	0.269
Ljung-Box test on the squared standardized residuals										
Lag	Q-stat.	P-value	Q-stat.	P-value	Q-stat.	P-value	Q-stat.	P-value	Q-stat.	P-value
5	0.683	0.984	0.914	0.969	6.500	0.261	4.692	0.455	1.763	0.881
10	2.228	0.994	1.448	0.999	12.181	0.273	7.729	0.655	3.585	0.964
15	3.588	0.999	2.082	1	18.648	0.230	8.198	0.916	6.139	0.977

Table A.4: Estimation results for the last 5 assets of the chosen models - Original train set

A.5 Plots and Figures - Test Set

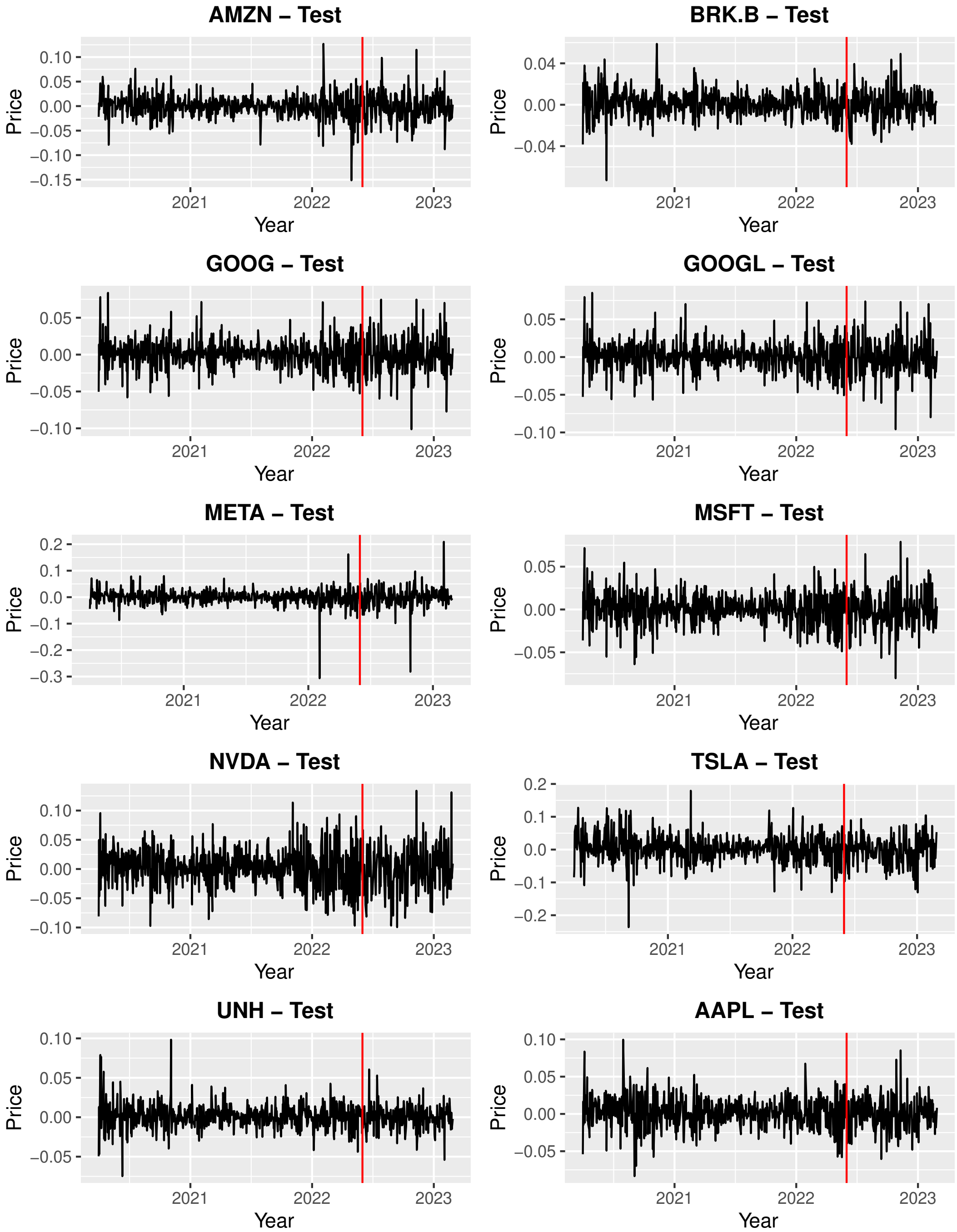

Figure A.3: Log-returns from 1st of April 2020 until 27th of February 2023. The red lines indicate the division between the train and test set.

Train Set	**AMZN**	**BRK.B**	**GOOG**	**GOOGL**	**META**	**MSFT**	**NVDA**	**TSLA**	**UNH**	**AAPL**
Mean	0.00037	0.00097	0.00119	0.00119	0.00026	0.00096	0.00184	0.00350	0.00122	0.00151
St. Deviation	0.0222	0.0122	0.0182	0.0184	0.0273	0.0174	0.0312	0.0416	0.0158	0.0200
95% VaR	-0.0315	-0.0190	-0.0309	-0.0312	-0.0399	-0.0294	-0.0517	-0.0605	-0.0240	-0.0311
99% VaR	-0.0660	-0.0263	-0.0482	-0.0479	-0.0651	-0.0445	-0.0756	-0.1000	-0.0363	-0.0535
Skewness	-0.4414	-0.0723	0.1273	0.1516	-2.1580	-0.1806	-0.0097	-0.1266	0.5801	0.0227
Excess Kurtosis	9.4994	6.2829	5.2893	5.2539	32.6309	4.2245	3.6809	5.8580	8.1612	5.2214
Jarque-Bera	1012	254	124	121	21,108	38	10	193	658	116
P-value	$< 2.2e^{-16}$	$< 2.2e^{-16}$	$< 2.2e^{-16}$	$< 2.2e^{-16}$	$< 2.2e^{-16}$	$< 2.2e^{-16}$	$< 2.2e^{-16}$	$< 2.2e^{-16}$	$< 2.2e^{-16}$	$< 2.2e^{-16}$
ADF test	-7.219	-6.751	-7.914	-7.878	-8.668	-7.570	-7.132	-7.770	-7.647	-8.202
P-value	0.01	0.01	0.01	0.01	0.01	0.01	0.01	0.01	0.01	0.01
Ljung-Box	16.297	11.693	27.148	27.845	20.789	39.003	18.301	11.127	18.647	11.67
P-value	0.2956	0.6309	0.0184	0.0149	0.1072	0.0004	0.1934	0.6761	0.1789	0.6328
Test Set	**AMZN**	**BRK.B**	**GOOG**	**GOOGL**	**META**	**MSFT**	**NVDA**	**TSLA**	**UNH**	**AAPL**
Mean	$-1.28e^{-3}$	$-1.88e^{-4}$	$-1.21e^{-3}$	$-1.22e^{-3}$	$-6.85e^{-4}$	$-4.29e^{-4}$	$1.19e^{-3}$	$-1.01e^{-3}$	$-1.42e^{-4}$	$-3.20e^{-5}$
St. Deviation	0.0288	0.0139	0.0250	0.0248	0.0395	0.0215	0.0373	0.0410	0.0148	0.0211
95% VaR	-0.0491	-0.0233	-0.0397	-0.0402	-0.0521	-0.0323	-0.0611	-0.0718	-0.0240	-0.0381
99% VaR	-0.0707	-0.0355	-0.0616	-0.0621	-0.0803	-0.0525	-0.0846	-0.0984	-0.0337	-0.0482
Skewness	0.3219	0.2730	-0.0275	-0.0142	-1.0876	0.1319	0.1511	-0.2501	0.1579	0.2044
Excess Kurtosis	4.5666	4.0797	4.7838	4.6031	18.8685	4.6133	3.9212	3.5687	5.1809	4.3880
Jarque-Bera	23.187	11.833	25.745	20.781	2073.7	21.601	7.5972	4.6363	39.252	16.924
P-value	$9.22e^{-6}$	0.0027	$2.57e^{-6}$	$3.07e^{-5}$	$< 2.2e^{-16}$	$2.04e^{-5}$	0.0224	0.0985	$3.00e^{-9}$	0.0002
ADF test	-6.0454	-5.7817	-6.2824	-6.3167	-5.8591	-6.2877	-6.0867	-4.3042	-5.8958	-5.0017
P-value	0.01	0.01	0.01	0.01	0.01	0.01	0.01	0.01	0.01	0.01
Ljung-Box	12.160	2.957	11.653	11.393	7.336	17.921	7.626	13.864	8.679	14.324
P-value	0.594	0.999	0.634	0.655	0.921	0.210	0.908	0.460	0.851	0.426

Table A.5: Descriptive statistics of the log-returns - Original test set

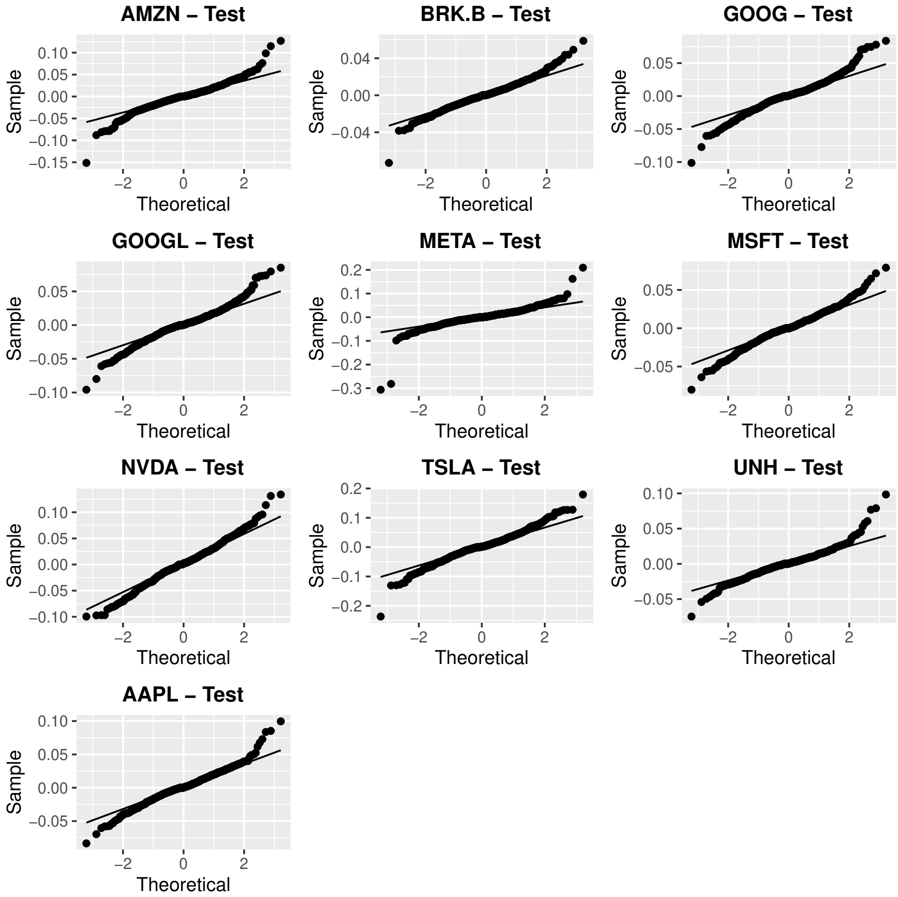

Figure A.4: Q-Q plots based on the original test set

Ljung-Box test on the squared residuals of the ARMA models										
	AMZN		**BRK.B**		**GOOG**		**GOOGL**		**META**	
Lag	ARMA(0,0)		ARMA(0,0)		ARMA(0,0)		ARMA(0,0)		ARMA(0,0)	
	Q-stat.	P-value	Q-stat.	P-value	Q-stat.	P-value	Q-stat.	P-value	Q-stat.	P-value
5	18.742	0.002	26.980	$5.8e^{-5}$	19.146	0.002	22.367	0.000	1.239	0.941
10	41.645	$8.7e^{-6}$	53.128	$7.0e^{-8}$	35.766	$9.2e^{-5}$	38.391	$3.2e^{-5}$	2.465	0.991
15	52.994	$3.9e^{-6}$	73.183	$1.2e^{-9}$	51.087	$8e^{-6}$	53.568	$3.1e^{-6}$	2.718	1
	MSFT		**NVDA**		**TSLA**		**UNH**		**AAPL**	
Lag	ARMA(0,0)		ARMA(0,0)		ARMA(0,0)		ARMA(0,0)		ARMA(0,0)	
	Q-stat.	P-value	Q-stat.	P-value	Q-stat.	P-value	Q-stat.	P-value	Q-stat.	P-value
5	34.380	$2e^{-6}$	46.874	$6.0e^{-9}$	16.386	0.006	57.808	$3.4e^{-11}$	40.978	$9.5e^{-8}$
10	61.259	$2.1e^{-9}$	105.78	$< 2.2e^{-16}$	51.470	$1.4e^{-7}$	82.584	$1.6e^{-13}$	67.111	$1.6e^{-10}$
15	80.918	$4.7e^{-11}$	152.94	$< 2.2e^{-16}$	75.255	$5.1e^{-10}$	94.750	$1.3e^{-13}$	79.736	$7.8e^{-11}$

Table A.6: Test for heteroskedasticity in the residuals of the ARMA models - Original test set

Parameter estimates for marginal distributions and statistic tests - the first 5 assets										
	AMZN		**BRK.B**		**GOOG**		**GOOGL**		**META**	
	ARMA(0,0)		ARMA(0,0)		ARMA(0,0)		ARMA(0,0)		ARMA(0,0)	
	Value	P-value	Value	P-value	Value	P-value	Value	P-value	Value	P-value
μ	0.001	0.221	0.001	0.047	0.002	0.001	0.002	0.002	0.001	0.130
ω	0.000	0.131	0.000	0.000	0.000	0.281	0.000	0.309	0.000	0.381
α	0.018	0.000	0.115	0.000	0.083	0.124	0.066	0.184	0.013	0.000
β	0.976	0.000	0.819	0.000	0.869	0.000	0.849	0.000	0.909	0.000
ν	5.109	0.000	7.076	0.000	3.296	0.000	3.502	0.000	5.020	0.000
Ljung-Box test on the standardized residuals										
Lag	Q-stat.	P-value	Q-stat.	P-value	Q-stat.	P-value	Q-stat.	P-value	Q-stat.	P-value
5	3.455	0.630	6.551	0.256	11.034	0.051	9.957	0.076	6.691	0.245
10	5.355	0.866	8.676	0.563	17.243	0.069	17.134	0.071	13.946	0.176
15	7.215	0.951	10.836	0.764	27.796	0.023	26.73	0.031	20.13	0.167
Ljung-Box test on the squared standardized residuals										
Lag	Q-stat.	P-value	Q-stat.	P-value	Q-stat.	P-value	Q-stat.	P-value	Q-stat.	P-value
5	4.131	0.531	0.613	0.987	4.598	0.467	6.386	0.270	3.828	0.574
10	6.138	0.804	4.498	0.922	9.051	0.527	10.327	0.412	8.929	0.539
15	12.451	0.645	6.230	0.976	16.268	0.364	16.748	0.334	14.307	0.502

Table A.7: Estimation results for the first 5 assets of the chosen models - Original test set

Parameter estimates for marginal distributions and statistic tests - the last 5 assets										
	MSFT		**NVDA**		**TSLA**		**UNH**		**AAPL**	
	ARMA(0,0)		ARMA(0,0)		ARMA(0,0)		ARMA(0,0)		ARMA(0,0)	
	Value	P-value	Value	P-value	Value	P-value	Value	P-value	Value	P-value
μ	0.002	0.005	0.003	0.004	0.003	0.012	0.001	0.101	0.002	0.004
ω	0.000	0.000	0.000	0.101	0.000	0.344	0.000	0.000	0.000	0.348
α	0.088	0.000	0.114	0.022	0.133	0.044	0.054	0.000	0.056	0.000
β	0.877	0.000	0.787	0.000	0.860	0.000	0.899	0.000	0.924	0.000
ν	5.315	0.000	7.354	0.002	4.477	0.000	4.087	0.000	5.895	0.000
Ljung-Box test on the standardized residuals										
Lag	Q-stat.	P-value	Q-stat.	P-value	Q-stat.	P-value	Q-stat.	P-value	Q-stat.	P-value
5	5.485	0.360	7.289	0.200	5.247	0.387	5.234	0.388	3.543	0.617
10	12.555	0.250	13.161	0.215	6.757	0.748	8.263	0.603	4.757	0.907
15	26.791	0.030	19.811	0.179	8.609	0.897	13.305	0.579	8.388	0.907
Ljung-Box test on the squared standardized residuals										
Lag	Q-stat.	P-value	Q-stat.	P-value	Q-stat.	P-value	Q-stat.	P-value	Q-stat.	P-value
5	3.509	0.610	3.663	0.599	0.674	0.984	5.044	0.411	1.578	0.904
10	6.024	0.813	14.167	0.166	3.958	0.949	5.800	0.832	11.783	0.300
15	9.650	0.841	16.346	0.360	11.101	0.745	6.855	0.962	12.903	0.610

Table A.8: Estimation results for the last 5 assets of the chosen models - Original test set

Bibliography

Abad et al., 2014. Pilar Abad, Sonia Benito Muela and Carmen Lopez. *The role of the loss function in Value-at-Risk comparisons*, 2014. URL https://www.researchgate.net/publication/289945405_The_role_of_the_loss_function_in_value-at-risk_comparisons.

Bilimoria, 2021. Dilshad Bilimoria. *How money maters and investing changed post Covid*-19, 2021. URL https://economictimes.indiatimes.com/mf/analysis/how-money-matters-and-investing-changed-post-covid-19/articleshow/81083658.cms?from=mdr.

Bluemel and Henley, 2021. James Bluemel and Alice Henley. *The virus that shook the world*, 2021. URL https://www.pbs.org/wgbh/frontline/documentary/the-virus-that-shook-the-world/.

Cherubini et al., 2004. Umberto Cherubini, Elisa Luciano and Walter Vecchiato. *Copula Methods in Finance*. John Wiley & Sons, Ltd., 2004. ISBN 00.470-86344-7.

Choudhry, 2013. Moorad Choudhry. *An Introduction to Value-at-Risk*. John Wiley & Sons, Ltd., 2013. ISBN 978-1-118-31672-6.

Economics, 2021. Copenhagen Economics. *Economic Consequences of the COVID*-19 *Pandemic*, 2021. URL https://copenhageneconomics.com/wp-content/uploads/2021/12/copenhagen-economics_economic-consequences-covid-19.pdf.

Elliott and Kopp, 2005. Robert J. Elliott and P. Ekkehard Kopp. *Mathematics of Financial Markets, Second Edition*. Springer Finance, 2005. ISBN 0-387-21292-2.

Fantazzini, 2008. Dean Fantazzini. *Dynamic Copula Modelling for Value at Risk*, 2008. URL https://papers.ssrn.com/sol3/papers.cfm?abstract_id=1542608.

Ghani and Rahim, 2018. I. M. Md Ghani and H. A. Rahim. *Modeling and Forecasting of Volatility using ARMA-GARCH: Case Study on Malaysia Natural Rubber Prices*, 2018. URL https://www.researchgate.net/publication/335431614_Modeling_and_Forecasting_of_Volatility_using_ARMA-GARCH_Case_Study_on_Malaysia_Natural_Rubber_Prices.

Hofert et al., 2018. Marius Hofert, Ivan Kojadinovic, Martin Mächler and Jun Yan. *Elements of Copula Modeling with R.* Springer, 2018. ISBN 978-3-319-89635-9.

Huang et al., 2009. Jen-Jsung Huang, Kuo-Jung Lee, Hueimei Liang and Wei-Fu Lin. *Estimating value at risk of portfolio by conditional copula-GARCH method*, 2009. URL `https://www.sciencedirect.com/science/article/pii/S0167668709001267`.

Huang and So, 2018. Jhe-Jheng Huang and Leh-Chyan So. *Application of Copula-GARCH to Estimate VaR of a Portfolio with Credit Default Swaps*, 2018.

Kelepouris and Kelepouris, 2019. Ionas Kelepouris and Dimos Kelepouris. *Value at Risk estimation using GARCH model*, 2019. URL `https://rpubs.com/ionaskel/VaR_Garch_market_risk`.

Kenton, 2023. Will Kenton. *S&P*500 *Index: What It's for and Why It's Important in Investing*, 2023. URL `https://www.investopedia.com/terms/s/sp500.asp`.

Kucharska and Pielaszkiewicz, 2009. Magdalena Kucharska and Jolanta Pielaszkiewicz. *NIG distribution in modeling stock returns with assumption about stochastic volatility - Estimation of parameters and application to VaR and ETL*, 2009. URL `https://www.diva-portal.org/smash/get/diva2:240092/FULLTEXT01.pdf`.

Kuester et al., 2006. Keith Kuester, Stefan Mittnik and Marc S. Paolella. *Value-at-Risk Prediction: A Comparison of Alternative Strategies*, 2006. URL `https://academic.oup.com/jfec/article/4/1/53/833052`.

Lin, 2021. Yaokun Lin. *Model Selection with AIC* & *BIC*, 2021. URL `https://machinelearningabc.medium.com/model-selection-with-aic-bic-10ac9dac4c5a`.

Lu et al., 2011. Xun Fa Lu, Kin Keung Lai and Liang Liang. *Portfolio value-at-risk estimation in energy futures markets with time-varying copula-GARCH model*, 2011. URL `https://link.springer.com/article/10.1007/s10479-011-0900-9`.

Nasdaq, 2023. Nasdaq. *SPX Historical Data*, 2023. URL `https://www.nasdaq.com/market-activity/index/spx/historical`.

Nelsen, 2006. Roger B. Nelsen. *An Introduction to Copulas.* Springer Series in Statistics, 2006. ISBN 0-387-28659-4.

Nugroho et al., 2019. D. B Nugroho, D Kurniawati, L. P Panjaitan, Z. Kholil, B. Susanto and L. R Sasongko. *Empirical performance of GARCH, GARCH-M, GJR-GARCH and log-GARCH models for returns volatility*, 2019. URL https://iopscience.iop.org/article/10.1088/1742-6596/1307/1/012003/pdf.

Pedersen, 2009. Jan Pedersen. *Lévy Processes*. Aarhus University, 2009.

Ruppert and Matteson, 2015. David Ruppert and David S. Matteson. *Statistics and Data Analysis for Financial Engineering - with R examples*. Springer Texts in Statistics, 2015. ISBN 978-1-4939-2614-5.

Sørensen, 2023. Kirstine Lykke Sørensen. *Master*, 2023. URL https://github.com/KirstineLykke/Master.

Wang et al., 2022. Yuling Wang, Yunshuang Xiang and Huan Zhang. *Comparison and Forecasting of VaR Models from Measuring Financial Risk: Evidence from China*, 2022. URL https://www.hindawi.com/journals/ddns/2022/5510721/.